UNIVERSITY OF KWAZULU-NATAL

COLLEGE OF AGRICULTURE, ENGINEERING AND SCIENCE

REDUCING NOISE FROM WIND TURBINES USING ACTIVE NOISE CONTROL

By

ADEWUMI GLORIA ADEDAYO

"Dissertation submitted in fulfilment of the academic requirements for the degree of Masters of Science in Mechanical Engineering"

Supervisor: DR FREDDIE L. INAMBAO

School of Engineering, Discipline of Mechanical Engineering,

Howard College, Durban.

November, 2014

“As the candidate’s supervisor I agree to the submission of this thesis”.

_____Dr Freddie Inambao_____ _____

NAME OF SUPERVISOR SIGNATURE

DECLARATION 1: PLAGIARISM

I, Adewumi, Gloria Adedayo declare that:

1. The research reported in this thesis, except where otherwise indicated, is my original research.
2. This thesis has not been submitted for any degree or examination at any other university.
3. This thesis does not contain other persons' data, pictures, graphs or other information, unless specifically acknowledged as being sourced from other persons.
4. This thesis does not contain other persons' writing, unless specifically acknowledged as being sourced from other researchers. Where other written sources have been quoted, then:

a. Their words have been re-written but the general information attributed to them has been referenced;

b. Where their exact words have been used, then their writing has been placed in italics and inside quotation marks, and referenced.

5. This thesis does not contain text, graphics or tables copied and pasted from the Internet, unless specifically acknowledged, and the source being detailed in the thesis and in the References sections.

Signed

27th February 2015

DECLARATION 2: PUBLICATIONS

DETAILS OF CONTRIBUTION TO PUBLICATIONS that form part and/or include research presented in this thesis (include publications in preparation, submitted, in press and published and give details of the contributions of each author to the experimental work and writing of each publication)

Publication 1: **Gloria Adewumi** and Freddie Inambao (2014). "Active Control of Wind Turbine Aerodynamic Noise Using FXLMS Algorithm" Proceedings of the 13th International Conference on Sustainable Energy Technologies 25th-28th August, 2014. HES-SO-Geneva-Switzerland (www.hes-so.ch/set2014).

Publication 2: **Gloria Adewumi,** Lumbumba T-E. Nyamayoka and Freddie L. Inambao (2014). Reducing Infra-sound and low-frequency noise from wind turbine blades and rotors using ANC. *Journal of Renewable Bio-resources* (accepted and awaiting publication).

In all these papers, I, Gloria Adewumi was the main and corresponding author, whilst Dr. Freddie Inambao was the co-author and research supervisor.

Signed

27th February 2015

ACKNOWLEDGEMENTS

I will like to convey my deepest gratitude to my supervisor Dr. Freddie Inambao who has been of immense help; offering guidance, support and assistance throughout the duration of this research.

I would also like to thank the staff of Sound and Vibration Research Group (SVRG) at the University of Stellenbosch and also the staff at the Vibration Research and Testing Centre (VRTC) at the University of KwaZulu-Natal for allowing me to use their noise measuring equipment while carrying out the study. Thanks also to Professor Maarten Kamper from the University of Stellenbosch, Cape Town, South Africa for allowing me to use the Mariendahl wind turbine in Stellenbosch for noise assessment.

Finally, my profound gratitude goes to my family who has supported me in every way possible and also my colleagues at the Green Energy Research Group for their contributions and advice.

ABSTRACT

Wind turbines while operating produce noise from the rotating mechanical parts and from the interaction of the blades with surrounding airflow. The noise produced by the blades consists of low frequency noise, airfoil self-noise and inflow turbulence noise. Active Noise Control (ANC) however, is a technique known to produce high level of attenuation in the low frequency range. The question therefore arose whether ANC can be used to reduce noise on wind turbines.

The MATLAB simulation investigated the primary objective which was to introduce an opposite phase that is generated and combined with the primary "anti-noise" wave through an appropriate array of secondary noise, developed using a set of adaptive algorithms which consequently results in cancellation of both noises. The MATLAB simulation also investigated three secondary objectives: (i) to use filtered-x least mean squared (FXLMS) feed-forward ANC; (ii) to use a Finite Impulse Response (FIR) adaptive filter structure; and (iii) to minimize residual noise which consequently leads to reduction in low frequency aerodynamic noise from wind turbines. Field measurement was carried out in order to achieve one secondary objective: (i) to measure noise emission from a test turbine facility.

Noise emission measurements were carried out at periods with the highest wind speeds which were between 10:00 am and 5:00 pm. Results show a reduction in sound pressure with increase in distance, with 64dBA at the foot of the tower and a sound pressure level of 54dBA at 30m away from the foot of the turbine. One-third octave analysis results indicate that although sound is attenuated with increasing distance, low frequency noise has higher frequency components having a value of 257Hz and a band power of 46dBA.

Active Noise Control Simulations using FXLMS algorithm was carried out using sampled noise at 22050Hz and for 2 seconds and combining the noise signal, the FXLMS filter and the primary path filter. The FIR filter was used for the primary propagation path and a reduction of noise by 29dB has been achieved.

TABLE OF CONTENTS

LIST OF FIGURES

LIST OF TABLES

NOMENCLATURE

Roman Symbols (Lower-case)

$a'(n)$ Filtered version of the reference input [-]

c Blade chord [-]

c_0 Speed of sound [m/s]

f_{peak} Peak energy [N]

f_z Axial pressure component acting on the rotor [N/m^2]

f_z^0 Circumferential average value of f_z [N/m^2]

h Trailing edge thickness [m]

$\acute{k}$ Corrected wavelength [m]

k Acoustic wave number

p Effective or root mean square sound pressure [Pa]

p_o Reference sound pressure (μPa)

q Dynamic pressure of the flow approaching blade tip [N/m^2]

r_e Distance between observer and airfoil trailing edge [m]

r_1, φ_1 Polar co-ordinates of the rotor plane [-]

r_1 Radial elements [-]

$s(n)$ Impulse response of the secondary path [-]

t Time [s]

$u(.)$ Input (or control) vector, $u(t) \in \mathbb{R}^p$

w Filter coefficients [-]

$w(.)$ Primary disturbance vector, $\dim[w(.)] = n \times 1$

$x(.)$ State vector, $x(t) \in \mathbb{R}^n$

$x(n)$ Vectors composed of the input-signals samples [-]

$y(.)$ Output vector, $y(t) \in \mathbb{R}^q$

Roman Symbols (Upper-case)

$A(.)$ State (or system) matrix, $\dim[A(.)] = n \times n$

A_s Acoustic area [m^2]

B Number of blades [-]

$B(.)$ Input matrix, $\dim[B(.)] = n \times 1$

C(s) Transfer function of the controller

$C(.)$ Output matrix, $\dim[C(.)] = 1 \times n$

D_R Diameter of rotor [m]

D_T Tower diameter [m]

$\dot{D}_h$ Directivity function [-]

$\check{E}(n)$ Instantaneous squared error

$\mathcal{F}_s\{.\}$ Fourier transformation with respect to the time s

G_1,G_2, G_3 are empirical functions [-]

G_4,G_5 Empirical functions of the parameters [-]

H Distance from ground to the center line of rotor shaft [m]

$\tilde{I}r$ Sound intensity [W/m^2]

K_c Low frequency correction [-]

$\mathcal{L}$ Turbulence length scale [-]

L Span of the airfoil [m]

L_p Sound pressure level [dB]

L_{pn} 12 sound pressure levels of the masking noise [Pa]

$L_{pn,avg}$ Energy average of the spectral lines identified as masking [Pa]

L_w Sound power level [dB]

L_{wd} Declared sound power level [dB]

L(s) Transfer function of the secondary source [-]

ΔL Blade segment semi-span [-]

M Mach number [-]

M(s) Transfer function of detector [-]

N Filter order and [-]

N(s) Transfer function of necessary electronics [-]

P Sound power of source [Watts]

P_o Reference sound power [Watts]

P(s) Primary source output [-]

Q_f Directivity factor [-]

R_{ref} Reference distance [m]

$(Re_c)_0$ Reference Reynolds number [-]

$S(n)$ Impulse response of the secondary path [-]

S(s) Secondary source output [-]

St' Strouhal number based on δ_p [-]

St'_p Peak Strouhal number [-]

St'' Strouhal number based on h [-]

St''_{peak} Peak Strouhal number [-]

T(s) Transfer function of path r_t [-]

U(s) Transfer function of path r_u [-]

V(s) Transfer function of path r_v [-]

W(s) Transfer function of path r_w [-]

Greek symbols (Lower-case)

α_s Time Fourier coefficient [-]

δ_p Boundary layer thickness for the pressure side [m];

δ^*_{avg} Average displacement for both sides of the airfoil [m];

θ Angle between blade chord line and source observer line [deg]

μ Step size of the algorithm which determines the stability and convergence of the [-]

ξ angle between the inverted local blade inflow velocity and the source observer line [deg]

ρ_0 Density [Kg/m^3]

σ Standard deviation for the declaration [-]

σ_p Standard deviation of production [-]

σ_R Estimate of the standard deviation of reproducibility [-]

φ Radial components [-]

φ angle between the plane of the blade and the plane containing chord line and observer [deg]

ω Temporal (radial) frequency [rad/s]

ω_1 Blade passage angular frequency [rad/s]

Greek symbols (Upper-case)

Δ Amount of delay in the secondary path [s]

Δ_{Ltn} Tonality [dB]

Ω Angular velocity of rotor [rad/s]

Ψ Angle between both airfoil surfaces [deg]

Superscripts

* Linear convolute operator

Subscripts

R Rotor

T Tower

c Correction

avg Average

ref Reference

p Pressure

Acronyms and abbreviations

ANC Active Noise Control

BPF Blade Passing Frequency

DSL Digital Subscriber Line

DSP Digital Signal Processing

FIR Finite Impulse Response

FXLMS Filtered-X Least Mean Square Algorithm

HAWT Horizontal Axis Wind Turbines

IEC International Electromechanical Commission

IIR Infinite Impulse Response

LMS Least Mean Square

MISO Multiple-Input Single-Output

MSE Mean Squared Error

NIMBY Not In My Backyard

PNC Passive Noise Control

SISO Single-Input Single-Output

SPL_l Sound pressure level of the laminar boundary layer vortex shedding noise [dB];

SPL_T Sound pressure level of the trailing-edge bluntness vortex shedding noise [dB];

VAWT Vertical Axis Wind Turbines

WLS Weighted Least Square

CHAPTER ONE
INTRODUCTION

1.1 General Introduction and Background of the Study

Cancelling out noise is based on the principle of destructive interference. When there is superposition between two sinusoidal waves, the resultant waveform is based on the frequency, amplitude and relative phase of the two waves. The source wave and its direct inverse interfering at the same time, leads to cancellation (Hansen and Snyder, 1997). Sounds travel in waveforms, which is similar to how ocean waves function. A wave cycle is one complete wave, made up of the peak and trough. Waves consist of amplitudes which represent the strength of a wave; higher amplitude means a higher peak and deeper trough.

When two waves strike each other, they combine and if their amplitudes are of the equal sign (either both negative and both positive) they will join up to become a single wave with a larger amplitude. This is referred to as constructive interference. On the other hand, if both amplitudes are of reverse signs, they will cancel out to form a wave with lesser amplitude, and destructive interference is produced. Sound and noise are relative and find their origin from the same phenomena of atmospheric fluctuations about the mean atmospheric pressure, as a result of variations in pressure fluctuations. Pure tones and other signals are deterministic, while noise is a stochastic or random phenomenon (Jacobsen *et al.*, 2007). Sound is convected by the wind, and it travels at a speed of approximately 340m/s. If the wind speed increases with an increase in height, then sound waves will travel faster than sound waves close to the ground, which results in the waves bending towards the ground. The degree to which the sound is enhanced or attenuated is affected by the power-law exponent, which is directly proportional to the effect of the wind (Tonin, 2012). Figure 1.1 shows wind speed profiles for a 10m high wind turbine.

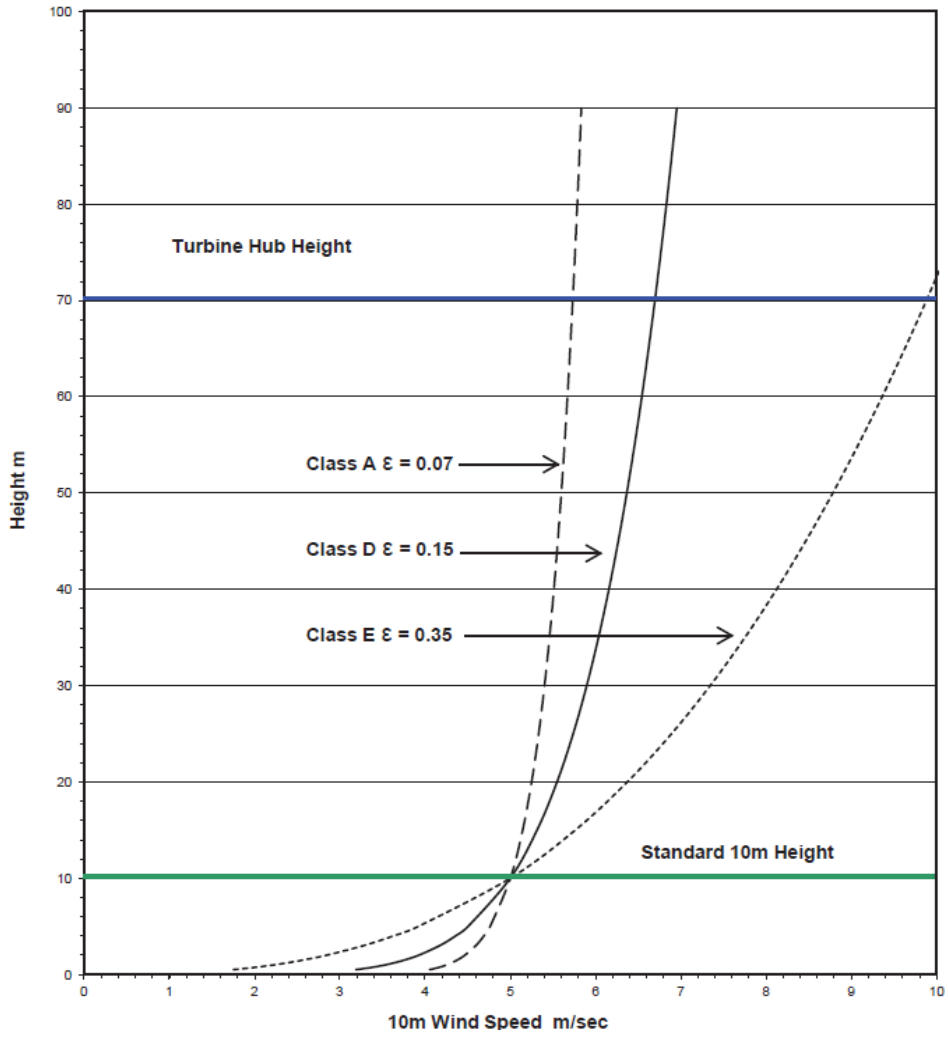

Figure1.1: Wind speed profiles for equal speeds of 5m/s for 10m height. Source: Tonin (2012)

Active noise control (ANC) is a method of noise reduction or control that works on the principle of destructive interference (Serizel *et al.*, 2012). The method is realized by superimposing created anti-noise with the noise to be cancelled (Akhtar *et al.*, 2005). Figure 1.2 shows the technique of destructive interference which is the backbone of active noise control (ANC). Various other components are needed for proper functioning of active noise cancellation. An externally placed microphone at a fixed position in the wind turbine is used to identify and acquire the noise coming from the blades reaction with the wind. The circuit will then generate an opposite signal that destructively interferes with the noise signal. The noise from the wind turbine, feeds the created wave in order for the created noise waves to destructively interfere (Narula *et al.*, 2012). The system is supplied by an external source of energy in order to function, hence the term "active noise cancellation"; active, meaning the

need for an external source. In summary, it occurs when another signal with an opposite phase but with the same amplitude with the original noise to be cancelled are made to destructively interfere with each other. Since wind turbines emit noise signals from the blades and rotors, the potentiality of applying ANC is studied and carried out in this work.

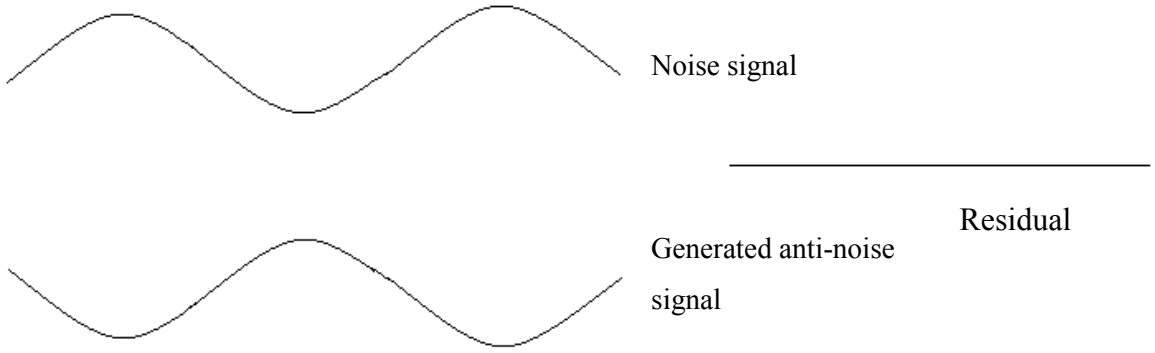

Figure1.2: Destructive Interference

Contemporary active noise control is normally accomplished through the use of analog circuits or digital signal processing (Zhu, 2009) in which adaptive algorithms are intended to study the waveform of the background noise, then based on the precise algorithm, produces a signal that will phase shift or reverse the polarity of the original signal (Kuo *et al.*, 1996). This reversed signal is then amplified and a sound wave is created by a transducer which is directly proportional to the amplitude of the source wave, and made to combine with each other. This successfully decreases the volume of the output noise (Kuo *et al.*, 1996).

A noise cancelling speaker should be in close proximity to the sound source to be attenuated. However, it is required that it contains similar audio power levels as the original noise to be cancelled (Hansen and Snyder, 1997). On the other hand, the transducer producing the cancellation signal may be placed with the sound source to be canceled. In the course of carrying out this research, the need to determine the tone levels, masking noise levels, tonality and declaration of sound power levels of the turbine will be required. Also, experiments will be carried out from which data for conclusion will be derived.

This dissertation will seek to find the extent to which the noise emanating from the blades and rotor of wind turbines can be reduced after placing the noise cancelling speaker close to the source of the noise. This was done by carrying out mainly simulations as the real life ANC was not built. The study also includes noise measurements from a 15kW horizontal

axis wind turbine in Stellenbosch, Cape Town, South Africa which was carried out to determine the amount of noise radiating in free field. Measurements were taken at a distance of 31.6m around the wind turbine. This was carried out according to IEC 61400-11 standard.

According to Arakawa *et al.* (2005), cancelling out noise in a wind farm has benefits of:

i. Making the operation of the wind farm convenient for personnel and those living around the wind farm
ii. Reducing noise that eliminates vibration which causes materials to wear out.

Mechanical noise is in relation with the gyration of the mechanical and electrical components and it produces tonal sounds which can be described as a hum or whine. This type of noise is developed from the relative movement of mechanical parts in the nacelle and the wind turbine tower (Rogers and Manwell, 2004) which includes:

i. Gearbox;
ii. Generator;
iii. Auxiliary equipment (e.g. hydraulics);
iv. Cooling fans; and
v. Yaw drives.

According to Doolan (2012), the major mechanical noises originate from the gearbox and external section of the blade tip. Present gearboxes on wind turbines are now made to be very quiet by introducing vibration damping methods (Rogers and Manwell, 2004) leaving the major noise sources on the blade. Mechanical noise can be conveyed and emitted by the rotor, hub and tower which may act as loudspeakers (Rogers and Manwell, 2004).

Aerodynamic noise on the other hand is as a result of the flow of air around the blades and is the major source of noise from the turbine (Lee *et al.*, 2013). Aerodynamic noise mostly increases with increased speed of the rotor and it produces a broadband noise which is usually described as “swishing” or “whooshing” sound (Jacobsen, 2005).

In general, there are six regions in which air foil self-noise is found on a blade (Jianu *et al*., 2012). Figure 1.3 is an air foil diagram showing the cross-section of a wind turbine blade and it explains the sources of noise as presented by Jianu *et al*. (2012). These regions include laminar boundary layer vortex shedding noise, turbulent boundary layer trailing edge noise,

trailing edge bluntness vortex shedding noise, separation stall noise, noise due to turbulent inflow and tip vortex formation noise.

These noises are composed of low frequency and high frequency tones. Several noise assessments have been carried out to determine the overall sound pressure level and also predictions to determine the various sources of noise (Baath, 2013; Rogers and Omer, 2012; Moriarty and Migliore, 2003). All these are carried out in order to develop technologies for their reduction. Reducing wind turbine noises helps produce a safer environment for humans and livestock and also reduces vibrations from the turbine which in turn reduces wear (Lopez-Caudana *et al.,* 2008).

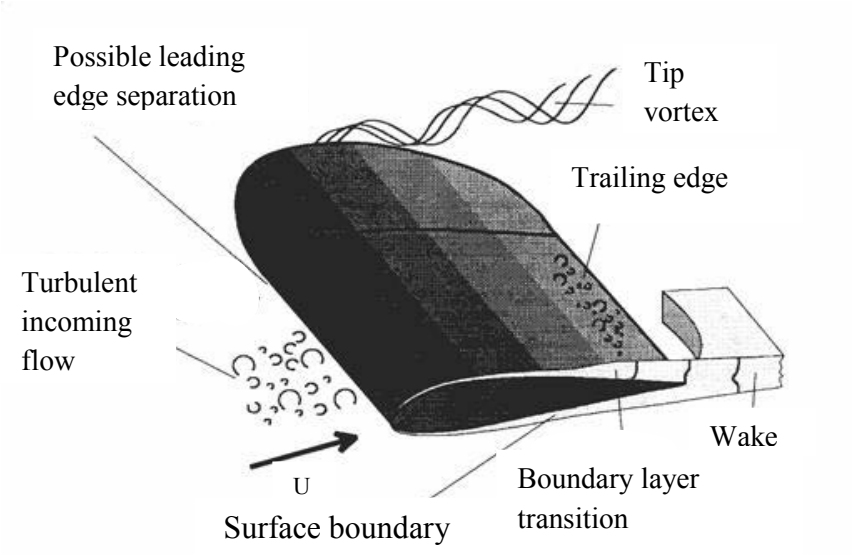

Figure 1.3: Sources of noise on a wind turbine blade (Rogers and Manwell, 2004)

Aerodynamic noises from the blades are aero acoustic and need a good understanding of blade aerodynamics. Turbulence exists forward of the rotating blade; interaction between the blade and turbulent eddies produces an unsteady lift which then creates a dipole-like noise source which found on the leading edge of the blade (Lloyd *et al.*, 2012). The type of noise formed is called inflow turbulence noise. When air flows over a blade surface, a boundary layer is created, and this is owing to the presence of viscous shear amid the blade and the air. The circumstances of flow on large wind turbine clarify this boundary layer will generally change to a turbulent form when the air finally reaches the trailing edge. This is known as trailing edge noise and has been said to be the major noise source on a wind turbine (Lee and Lee, 2014). The directivity pattern of a trailing edge noise is an important quality, which is unlike a monopole or dipole. Most of the sound is emitted frontward of the blade in the

direction of rotation (cardioid directivity pattern) (Oerlemans *et al.*, 2009), leaving little to be radiated behind. This clarifies the "swish" character of wind turbine noise in which an observer on the ground will occasionally receive variations in acoustic energy during blade rotation. Another important source of noise from wind turbines occurs from the interaction between rotating blades and the tower (Moriarty and Migliore, 2003); this design of wind turbines had the rotors placed downwind, which produced noise. Rotor placements of newer designs of wind turbines are usually upwind of the tower, thus removing the interaction between the wake and rotor. The blades however, still come across an area of disturbed flow which leads to noise production (Laratro *et al.*, 2014).

The rapid growth and widespread use of wind energy around the world have prompted more questions on noise and its corresponding effects on humans living around it and the environment. It has been established that the annoyance perception people have about wind turbines is seemingly related to specific aspects, such as the general perception people have about wind power generation, their opinion about wind turbines (e.g. landscape impact) and whether there was an economic interest attached to them at all (Arezes *et al.*, 2014). Parts of the study found out that some of the people who stayed in rural settlements were proud of wind turbines being in their backyards since it was gaining acceptance globally due to the green and clean energy produced by them. In addition they believed it had economic advantage as people visited the community more because of the turbines that were built which often lead to a corresponding increase in local commercial activities (Arezes *et al.*, 2014).

The occurrence of noise depends on the level of acoustic emission of the turbine and secondly on the distance between the turbine and nearest residences (Jianu *et al.*, 2012).

1.2 Development in Wind Turbine Technology and their Classifications

Wind machines have been in existence as far as 200 B.C and they were first used in Persia (present day Iran) for pumping water, sawing wood, grinding and pumping air for a failing organ (Shepherd, 1990). They were originally seen in Europe during the Middle Ages and used in England around the 11^{th} or 12^{th} century (Shepherd, 1990). The Scottish, scholar James Blyth installed a battery charging machine using the first electricity generating wind turbine (Shepherd, 1990). It was to light his holiday home in Mary Kirk in Scotland. Wind technology was later revived by the evolution and propagation of electricity and the

engineering science of Aerodynamics. Wind machines were initially built from wood throughout North-West Europe and by the beginning of the twentieth century; they were still in use in Germany (Shepherd, 1990).

Beginning from the nineteenth century, wind technologies became more popular as they were used for irrigation and were built of sheet with about 20 blades and were mostly used in the field of agriculture (Heier, 2006).

Man has continuously sought for ways to improve his existence and sustenance; this he has done using technologies to improve his means of transportation, communication, health, agriculture and power. The basis of these is energy production, conservation and transformation. As the population of mankind increased, there was also a direct corresponding increase in the demand for energy. The use of coal, gas, oil and other non-renewable means for the generation of energy is fast becoming unpopular because of the pollution they cause and also most importantly the damage to the environment, as fossil fuels contribute to global warming. However, according to the United States Department of Energy, wind energy has benefits of being an inexhaustible green energy source; do not consume water, clean, cost effective and above all sustainable.

Wind turbines can be classified based on their rotor shaft placement as vertical axis wind turbines (VAWT) and horizontal axis wind turbine (HAWT). In the HAWT, the central rotor shaft and the electric generator are placed at the top of a tower pointing into the wind while the VAWT have their main rotor shaft set vertically (Abdullah and Fekih, 2013). VAWT are further classified based on their rotor types into lift and drag type (Pearson, 2013). The drag type rotors function due to greater drag force on one side of the rotor axis while lift-type rotors generate lift by using airfoil shaped blades and these types have higher efficiency than the drag type (Pearson, 2013). VAWT tend to be more influenced by the wake from the upstream blades. An advantage of VAWT is their ability to catch wind from all directions eliminating the need for a yaw mechanism (Pearson, 2013). They are also not built as high as HAWT which makes them less visible and can therefore withstand extreme weather conditions (Ragheb, 2013). Figure 1.4 shows a HAWT and VAWT.

Figure1.4: Horizontal axis wind turbine (HAWT) and vertical axis wind turbine (VAWT)

1.3 Statement of the Problem

Because of the noise they emitted by wind turbines, they are not built near residential homes. Mechanical noise is generated from the interactive movements of mechanical parts and their dynamical response (Arakawa *et al.,* 2005). On the other hand, aerodynamic noise stems from airflow around the blades; it occurs as the blades encounter turbulence with the passing air. Various researches (Jianu *et al.*, 2012; Arakawa *et al.*, 2005; Klug, 2002) have indicated that this noise type is the prevailing cause of noise from wind turbines. Wind turbine noise is not known to cause a loss in hearing but they produce low frequency noise and vibration which may have adverse health effect on humans (Jakobsen, 2005); one of this is "blade thump" noise which leads to a health condition known as "wind turbine syndrome". The following are the symptoms:

i. Dizziness;
ii. Sleep disturbance;
iii. Problems with concentration and memory.
iv. Headache;
v. Visual blurring;
vi. Vertigo;

vii. Nausea;
viii. Rapid heart rate; and
ix. Ringing or buzzing in the ear;
x. Irritability

1.4 Limitation of the Study

While conducting the study, there were some uncertainties as to how ANC could be used on wind turbines since unlike past approaches where ANC's were used in ducts and in fans, the present studies are considering using ANC in free field. This could be a challenge because the blades are rotating in free and open field and blade interaction with atmospheric turbulence produces noise due to various mechanisms. The noises are from the tip, interaction of the blade with turbulence and passage of blade behind the tower. All these result in the issue of controlling noise actively on wind turbines more complicated than noise from a duct or from an enclosed fan.

The dissertation will focus on horizontal axis wind turbines and noise measurements are carried out in accordance with IEC 61400-11- Small wind turbines.

The noise measurements will be limited to a fixed speed wind turbine in Stellenbosch, located in Cape Town, South Africa and to the parameters that applied at the particular time the measurements were carried out. Noise measurements will be limited to seven hours during the day when the wind speed is at its peak.

The algorithm used is limited to Filtered-X Least Mean Squared (FXLMS) algorithm and control of noise was limited to simulations carried out using noise signal from a wind turbine.

1.5 Research Question

The following are the basic questions to be dealt with:

i. What are the challenges of using an Active Noise Control (ANC)?
ii. Which type of control system will be used?
iii. Which adaptive filter structure will be used?
iv. What systems ANC has been used on?

To help answer these questions effectively, a good knowledge of aerodynamic noise on wind blade and an in-depth understanding of Digital Signal Processing will be required.

1.6 Research Objectives

The primary objective of this research is to introduce an opposite phase that is generated and combined with the primary "anti-noise" wave through an appropriate array of secondary noise, developed using a set of adaptive algorithms which consequently results in cancellation of both noises.

The secondary objectives are:

i. To measure noise emission from a test turbine facility
ii. To use FXLMS Feed-forward ANC;
iii. To use a Finite Impulse Response (FIR) adaptive filter structure;
iv. To minimize residual noise which consequently leads to reduction of low frequency aerodynamic noise from wind turbines

1.7 Statement of the Research

The study aims at investigating noise reduction in wind turbines using Active Noise Control.

1.8 Significance of the Study

This research intends to draw attention to the possibility of implementing Active Noise Control in wind turbines. Moreover, this study will benefit individuals dwelling around wind turbine plants and also for wind turbine manufacturers. Siting of wind turbines far away from human dwelling because of the noise disturbance will no longer be necessary. The cost of connection to the grid and cost of transportation in the case of maintenance and repairs will be reduced due to proximity to the grid.

If noise from wind turbines is properly controlled, it could potentially contribute to the widespread acceptance of wind turbine technology thereby reducing overdependence on fossil fuels and other non-renewable energy sources. This way our planet is safe and there are lesser carbon emissions

Reducing or cancelling out aerodynamic noise from wind turbines will benefit humans and animals living close to wind farms. It will increase the widespread acceptance of wind turbine technology for power generation and the issue of "Not in My Backyard (NIMBY)" will be minimized. Wearing of materials will also be reduced as noise reduction will result in vibration control. This would be a breakthrough in the area of renewable energy technologies.

Finally, there is a scarcity of literature on the use of ANC's in wind turbines as a whole (rotor blades, wind turbine generators and wind turbine transformers). It is hoped that this research thus contributes to knowledge creation in these areas.

1.9 Definition of Terms

Aerodynamic noise: This is variation in fluid pressure when air passes over a streamlined body.

A-weighted: A screen applied at each frequency to give a near estimate of how the human ear responds to frequency variations.

Amplitude: The comparative affiliation represented on a gauge of -1 to 1 between the difference in localized air pressure and the ambient atmospheric air pressure.

Background Noise: This is the sound pressure of the surrounding background.

Broadband Noise: A noise which is made up of peak frequencies that take place in more than one third-octave bandwidths.

Decibel (dB): A unit for the expression of sound wave intensity, and it is 20 times the logarithm to the base of ten of the pressure ratio emitted by the sound wave to a referenced pressure of 0.0002 Pascal.

Equalized Sound Pressure Level (Leq): The root-mean-squared rate of sound energy in a given segment derived while the wind turbine is working and before subtracting the background noise.

Fast Fourier Transform (FFT): A process for calculating the Fourier transform of a set of discrete data. It is an analysis utilized to derive the sound pressure levels at varying frequencies that add to the total sound over the studied section.

Hertz (Hz): The International Standard unit of frequency, equivalent to one cycle per second.

Hub Height: The height from the foot of the wind turbine to the center of the wind turbine rotor.

Low Frequency Sound: Refers to sound in the frequency range 20Hz – 500Hz.

Narrowband Noise: A noise which is composed of one or several peak frequencies all taking place in the same one-third-octave bandwidth.

One-Third-Octave Bandwidth Analysis: A sound analysis of a noise sample that indicates the level of sound pressure in each progressive one-third-octave.

Pascal: The International Standard of reference pressure equivalent to one Newton per metre squared.

Peaks / Bandwidth: Concentrated sound pressure in frequencies radiated by a wind turbine.

Sound Power Level: The derived value of sound pressure radiated at a source location

Sound Pressure Level (SPL) – the quantity of sound pressure experienced by a receiver at a stated distance from the sound source.

Wind Turbine Noise: The acoustic sound radiated from a point or several points from a wind turbine.

Wind Turbine Sound: The overall sound pressure radiated from an operating wind turbine stretching from frequencies 20 Hz – 20000 Hz.

1.10 Scope of the Work and Thesis Outline

The scope of this research work is to investigate the residual noise output when Active Noise Control is applied on a wind turbine blade in operation. The investigation includes sound pressure level measurements; site conditions and position of microphone for noise emission measurements. These investigations were performed to gain knowledge of which frequency range the blades generate the most noise, what type of ANC would be feasible to use, and where to install it.

Furthermore, the scope was to implement feed-forward active noise control system with one reference microphone and one error microphone. This was implemented using the necessary

parameters and at different positions to attenuate the acoustic noise and obtain lower noise levels.

The dissertation consists of six chapters.

Chapter one introduces the aims, objectives and general background of the study.

Chapter two provides some theoretical information about the acoustic wave equation, sound directivity and the nature of noise in wind turbines. Active Noise Control system is also introduced.

Chapter three analyses the problem of wind turbine noise and their root causes.

Chapter four presents the Methodology and the procedure for measurement of primary noise at several points around the wind turbine.

Chapter five presents the results and analyses the MATLAB simulation results to observe how the noise cancels out.

Chapter six summarizes the conclusions and future works.

CHAPTER TWO
LITERATURE REVIEW

2.1 Introduction

This chapter presents extensive literature survey about various research studies and applications as regards noise reduction from wind turbines. Noise from wind turbines are radiated forward and the intensity varies at different locations around the wind turbine. Altering the airfoil shape, adding of serrations, replacing existing airfoils with silent ones and reducing rotor revolutions per minute (rpm) are some of the methods that are being currently applied for noise reduction. However, they have limitations of reducing power output and needing a lot of cost for maintenance.

This review exposes the constraints and gaps within the field of acoustics as it relates to wind turbine applications as some of these passive methods were only successful at achieving noise reduction of the high frequency noise and not being able to work on the low frequency components.

Recent trends and progress made in the field of ANC in reducing low frequency noise have been studied. This is possible because of the advancement in the area of digital signal processing technology. For noise cancellation to occur, it is required that the wave must be precisely 180^{o} out of phase while maintain the same amplitude. The studies shows that ANC have worked well in reducing impulsive noise, chaotic noise, broadband noise and narrowband noise.

2.2 The Acoustic Wave Equation

One of the characteristics of fluids is their lack of constraint to deformation and they lack the ability to transmit shearing force due to the force of inertia and also react to changes in shape (Jacobsen *et al.*, 2011). The wave equation can be derived from the conservation of mass principle and momentum equation. From the conservation of mass principle and Euler's equation of state, the acoustic wave equation is derived using the vector representation in Figure 2.1 and given by Jacobsen *et al.* (2011) as:

$\nabla^2 p(x,s) - \frac{1}{c^2}\frac{\partial}{\partial s^2} p(x,s) = 0$ (2.1)

where ∇^2 = Laplace operator, $\nabla^2 = \Delta[AW01]$

The wave equation can be described in frequency domain by the application of Fourier transformation of acoustic pressure p(x, s). The Fourier transform also given by Jacobsen *et al,* (2011) is:

$P(x,\omega) = \mathcal{F}_s\{p(x,s)\} = \int_{-\infty}^{\infty} p(x,s) e^{-jws} ds$ (2.2)

$P(x,s) = \mathcal{F}_s^{-1}\{p(x,\omega)\} = \frac{1}{2\pi} \int_{-\infty}^{\infty} p(x,\omega) e^{jwt} ds$ (2.3)

where:

$\omega = 2\pi f$ denotes the temporal (radial) frequency,

$\mathcal{F}_s\{.\}$ Fourier transformation with respect to the time s

In the frequency domain, the wave equation can also be given as:

$\nabla^2 p(x, \omega) + \left(\frac{\omega}{c}\right)^2 p(x, \omega) = 0$ (2.4)

This form is known as the Helmholtz equation. Where ω/c denotes the acoustic wave number *k*.

$k^2 = k^2(\omega) = \left(\frac{\omega}{c}\right)^2$ (2.5)

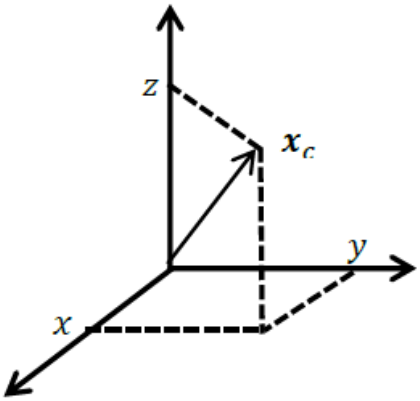

Figure 2.1: Illustration of solution of the wave equation in Cartesian co-ordinates (Jacobsen *et al.*, 2011)

2.3 Sound Directivity

Most of the sound in a wind turbine is radiated forward of the blade in what is referred to as cardioid directivity pattern (Lee *et al.*, 2013). The directivity function for wind turbine trailing edge noise established by Brooks and Burley (2001) is given as:

$$D = \frac{2\,sin^2(\frac{\theta}{2})sin^2\varphi}{(1-Mcos(\xi)^4} \tag{2.6}$$

where:

Θ Angle between the source observer line and the blade chord line [degrees];

φ Angle between the plane containing chord line and observer and the plane of the blade [degrees];

ξ Angle between the inverted local blade inflow velocity and the source observer line [degrees]; and

M Local blade inflow Mach number [-].

The directivity of sound explains that there is a significant variation in the strength of sound level emission from a source and is dependent on the varying directions from the source of the sound. It can be measured in either directivity index in decibels or as a dimensionless value, Q. Friman (2011), in his studies investigated the aerodynamic sources from the rotor blades and these sources which are induced by flow are expected to have a dipole character of

directivity and it was established that since the directivity factor of a source is sound intensity on the axis in the far field, normalized by the intensity of sound of an Omni-directional source with the same sound power, then:

$$\tilde{I}r = \frac{1}{2}\rho ck^2\left(\frac{|Q|}{2\pi r}\right)^2 \quad (2.7)$$

and directivity factor:

$$Q(f) = \frac{(K_a)^2}{R_1} \quad (2.8)$$

Sound power level is the property of the sound source and it provides the total acoustic power emitted by the wind turbine blade (source of noise); while sound pressure is a property of sound at a given observer location (Rogers and Manwell, 2002; Jacobsen *et al.*, 2011)
Sound Power level of a source is given as:

$$L_w = 10log\left(\frac{P}{P_0}\right) \quad (2.9)$$

where:

P Sound power of source [Watts];

P_0 Reference sound power [10^{-12} Watts];

Sound Pressure Level (SPL) in decibels dB is given by:

$$L_p = 20log\left(\frac{p}{p_0}\right) \quad (2.10)$$

where:

p Effective or root mean square sound pressure [Pa]; and

p_0 Reference sound pressure [20μPa] (Swift-Hook, 1989).

There are usually some variations in noise from wind turbines as wind turbulence varies. Turbulence in the ground level wind will affects an observer's ability to hear other noises. An observer at the bottom of the turbine will discover there are instants when noise from wind turbine was perceived over the background noise (Rogers and Manwell, 2004).

2.4 Passive Approaches to Noise Reduction in Wind Turbines

The noise emitted from wind turbines is a strong area of research. So far, a lot of attention has been given to passive approach of noise control (Göçmen and Özerdem, 2012; Jianu *et al.*, 2012; Oerlemans *et al.*, 2009). Some of the passive approaches include adjusting of airfoil shape by changing the shape of the pressure side and it includes the design of thinner trailing edges and engraved surfaces at the downward part of the airfoil (Göçmen and Özerdem, 2012), and this can be carried out without a loss in the aerodynamic performance. However, in the case of an acoustically optimized airfoil shape, it should be noted that trailing-edge noise is reduced by changing the structure of the boundary layer turbulence (Oerlemans *et al.*, 2009). It was considered that improvements can be carried out on airfoils that are commercially to emit lesser self-noise and thereby having a enhanced aerodynamic performance. This approach reduced noise by up to 5dB.

Investigations in a number of experimental studies on 2-D airfoils, model wind turbines and full scale wind turbine shows that attenuations to noise level were obtained by the use of serrations of saw-tooth profile with edges inclined at less than 45 degrees to the direction of mean flow (Howe, 1991). The serrations were able to decrease noise by roughly 3dB at low frequencies.

Other studies have been carried out which indicated that to prevent increased noise at high frequencies, it is critical to align the plane of the serrations with the trailing edge flow (Oerlemans *et al.,* 2009).

The use of silent airfoils which replaced airfoils existing in the external region of a baseline blade in the zones of highest flow velocities and peak aero-acoustics noise levels was conducted by Scheppers (2007), and was called the SIROCCO project; it aimed at modifying blades with an outer region which had different trailing edges, so designing a new airfoil would result in improved performance. However, studies carried out by Oerlemans *et al*. (2009), explain that the SIROCCO blade could only reduce noise by up to 0.5dB, probably because the brushes were too short, or possibly the constituent materials had low efficiency. Further studies (Jianu *et al.,* 2012; Oerlemans *et al.,* 2009) indicated that the serrated blade and blade with trailing edge brushes showed tip noise at high frequencies, which is mainly radiated during the upwind part of the revolution and it was most important at low wind speed due to high tip loading.

Other passive approaches include reducing rotor revolution per minute (rpm) or rotor diameter and increasing blade pitch (Oerlemans *et al.*, 2009; Rogers and Manwell, 2004). This method was not appropriate because of its limitation as a result of decrease in the angle of attack. Oerlemans (2011) in his study of the flow around a wind turbine blade explained that lower angle of attack resulted in a lower reaction force and therefore a lower torque. This consequently explains the overall loss in power output (Jianu *et al.*, 2012).

A numerical approach, carried out by Arakawa *et al.* (2005) showed that the use of pressure fluctuation analysis indicated that the actual tip shape shows increased frequency pressure fluctuations which were not present for the ogee type tip shape. Results from the analysis have indicated noise reduction in the use of an ogee type tip shape with frequencies above 3kHz by up to 5dB. Overall reduction was found to be 2dB.

Experiment on the minor modification of porous airfoils was carried out by Geyer (2010). The idea was modelled after the wings of a bat where the surface roughness provided by the porous material ensured the existence of a turbulent boundary layer. A sound reduction of up to 10dB and more was measured. This measurement was taken at low and medium frequencies. But had limitations of accumulated dirt in the pores and this led to frequent costly maintenance.

Leloudas *et al.* (2007) performed noise measurements on Siemens SWT-2.3-93 wind turbine and they observed that at constant rotational speed, the noise increased as the pitch angle decreased and most of the noise was generated at the tip, where the velocities were at the maximum. Therefore, a balance for a perfect pitch angle and rotational velocity at which the lowest noise is emitted is sought. This is done by constraining the power loss that would be traded for the noise reduction.

Noise from wind turbines vary as changes occur in the rotor due to turbulence in the wind. Figure 2.2 shows various wind profiles for equal wind speeds of 5m/s for 10m high towers.

2.5 Active Noise Control Systems

An important reason why active noise control (ANC) is more important than passive noise control (PNC) at low frequencies (Mudallah and Mohammed, 2008; Kottayi and Narayanan, 2012) is that ANC uses a digital signal processing (DSP) system as the canceler, which can execute complicated mathematical operations with enough speed and precision in real time

(Zhu, 2009). An in-depth review of the various ANC systems in the last seven and half decades was carried out by George and Panda, (2013) with emphasis on non-linear techniques. ANC systems have the advantage of being small, compact, environmentally adjustable, and they are cost effective (Hashemian, 1996).

The two main criteria to be fulfilled for an ANC system to function properly are: (i) the anti-noise wave must be similar in frequency and shape to the noise wave and they must be exactly 180^{o} out of phase in reference to the source noise wave, when reaching the target area (Hansen and Snyder, 1997; Hashemian, 1996), or else a second acoustic noise is generated. For a very efficient cancelling system, the source noise must be almost stationary in relative to the secondary speaker radiating the counter wave; (ii) the source of noise should be in close proximity to the ANC system and for best results, the target noise should be mainly radiating in one direction (Hashemian, 1996).

ANC systems can be broadly classified into Feed-forward and Feed-back control (George and Panda, 2013), or a combination of hybrid ANC (Kuo *et al.*, 1999; Lopez-Caudana *et al.*, 2008). Depending on the noise signal and environmental characteristics, they both have their advantage and disadvantages (Behera *et al.*, 2013; Chang and Luoh, 2007).

An ANC has to be adaptive due to environmental changes, system component degradation and noise source alteration (Chang and Luoh, 2007). ANCs are generally designed on the basis of a mathematical description and its linearized model (Chang and Luoh, 2007). Acoustic delay is also a factor that must be sufficiently dealt with in a noise cancelling system (Hashemian, 1996).

The applications of ANC can be seen in a high-speed elevator in which various transfer paths of noise are transmitted from motor and rope to cabin interior. A model of multiple-input and single-output (MISO) with respect to transfer paths of a high-speed elevator on conditions of stationary and driving states was built. A modified algorithm was developed and applied to the elevator system in order to improve the active noise control performance. A noise reduction of 8dB was achieved in the cabin at ear level (Yang *et al.,* 2013).

ANC was also applied to impulsive noise which occurs in channels which suffer from switching, manual interruptions, ignition noise and lightning, for example Digital Subscriber Line systems (DSL) and digital TV (Zahedpour *et al.*, 2009), and the focus of the author was on removing additive impulsive noise from a low pass signal. An iterative method where the

initial detection of the impulsive noise locations is performed using an adaptive thresh-holding technique (Sun *et al.*, 2005).

An investigation on the effect of using an ANC system on a radial fan was carried out by Muddala and Mohamed (2008). Sound levels at different positions were measured and a suitable position was selected. Their investigations included power spectral density measurements, sound pressure level measurements and octave band measurements. A single channel feed-forward ANC system was used and effective on the studied ventilation system using duct with an airflow speed of 4-5m/s. Noise reductions between 20-30dB for the tonal components and 5-10dB for broadband noise in the frequency range of about 100Hz and 200Hz were achieved respectively.

Gérard *et al.* (2005a) dealt with the control of noise from engine cooling fans radiating noise in free-field at the first harmonics of the blade Passing Frequency (BPF) (Figure 2.2), using a single-input single-output (SISO) adaptive feed-forward controller was implemented. The validity of the model was used for the fan noise only when the highest radiating modal component of the flow is taken into account and this was first derived and combined with a model for loudspeaker radiation. The performance of the approach was assessed using three metrics for global control (Gérard *et al.=,* 2005a). The ability of the ANC system to significantly reduce the BPF and its first harmonics in free field was clearly demonstrated and the tones at the BPF and its first harmonic are attenuated by up to 28 and 18dB respectively.

Global reduction of axial-flow fan noise in ducts using hybrid Passive-Active Noise Control was studied by Wong *et al*. (2003). A typical adaptive feed-forward control system was the ANC used.

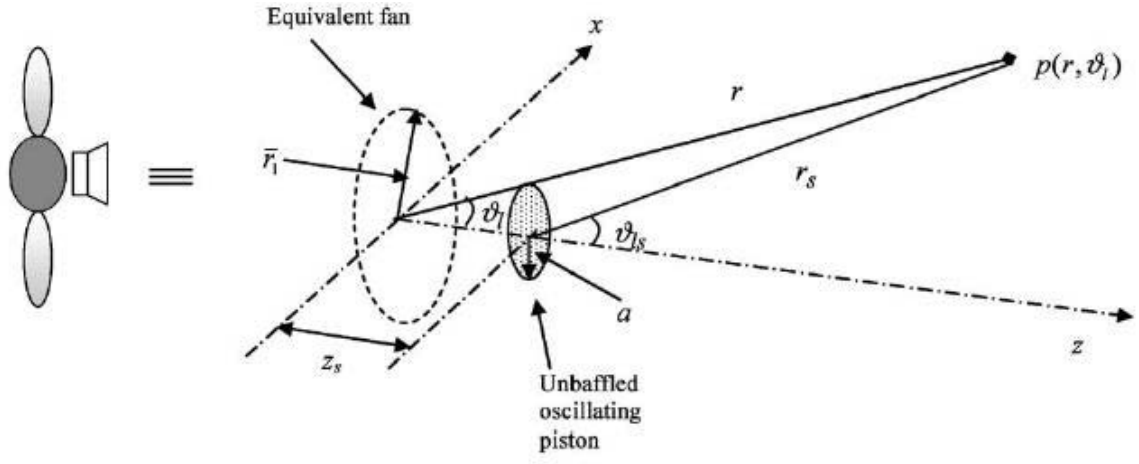

Figure 2.2: Active noise control arrangement for a free-field fan noise (Gérard et al., 2005a)

Two types of reference sensors were used: an infra-red device and a microphone. One sensor was used as reference at a time in order to compare their effectiveness. Using the infra-red as a reference sensor eliminated the problem of acoustic feedback and ensured that the system was stable. The aerodynamic pressure which fan blades employ on the fluid were broken down into an axial (z) component related to the thrust and a circumferential component related to the drag as depicted in Figure 2.3. The time Fourier series is given by Gérard *et al.* (2005b) as:

$$f_z(t: r_1, \varphi_1) = \sum_{s=-\infty}^{+\infty} A_s(r_1) e^{-is\omega_1\left(t-\frac{\varphi}{\Omega}\right)} = f_z^0(r_1) \sum_{s=-\infty}^{+\infty} \alpha_s(r_1) e^{isB\varphi_1} e^{-is\omega_1 t} \qquad (2.11)$$

where:

f_z Axial pressure component acting on the rotor [N/m^2];

t Time [s];

r_1, φ_1 Polar co-ordinates of the rotor plane [-];

A_s Acoustic area [m^2];

r_1 Radial elements [-];

φ Radial components [-];

Ω Angular velocity of rotor [rad/s];

f_z^0 Circumferential average value of f_z [-];

B Number of blades [-];

α_s Time Fourier coefficient [-]; and

ω_1 Blade passage angular frequency [-].

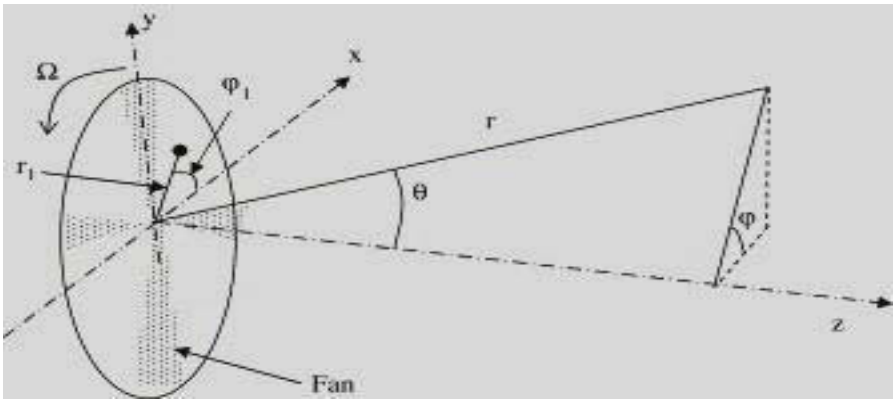

Figure 2.3: Radiation of sound from an axial fan into free field (Gérard *et al.,* 2005b)

The authors concluded that passive control methods can be used to attenuate broadband components of fan noise and the high level of low frequency discrete fan noise can be globally reduced by using ANC. An overall noise reduction of about 6dB was achieved.

Attempts have been made to reduce noise from exhaust stacks with spray dryers of large-diameter (Li *et al.,* 2006), using in-duct control sources and error sensors. The effect of the location of error sensors on the active control of tonal noise was evaluated by locating the control speakers optimally. The use of experiments showed that ANC can always bring about cancellation at the error sensor location. When the error sensors are located optimally, there is noise reduction in the far-field noise due to a consequence of minimization of the sound field at the error sensor location. The results from using optimized ANC system showed that the tonal noise emitted from the exhaust stack was minimized to almost the background noise level.

Investigation for turbofan engine noise using ANC was carried out by Dennis (2007) where a fan rig called "Advanced noise control fan" was designed and implemented in a range of experiments. The actuators to carry out the noise control were attached inside stator vanes and on fan duct walls. A number of tests were performed to show multiple and single duct mode cancellation from the exhaust and inlet of the fan duct. The author went on to state that

there was lesser need to concentrate on Active Noise Control of Turbofan engine noise because newer engine cycles are becoming less tone dominant except that they are methods for reducing broadband noise.

Lauchle *et al.* (1997) researched the use of ANC to reduce noise in a discrete-frequency axial flow fan. Here the fan itself is used as the source of the anti-noise. This was accomplished by driving the entire fan unit with an electro-dynamic shaker, which transforms the fan into a crude loudspeaker. A Feed-forward FXLMS algorithm was used and an excellent global noise reduction was achieved. At the error sensor location, fundamental blade-passage frequency sound pressure level is reduced by 20dB while the second harmonic level and third harmonic level are reduced by 15dB and 8dB respectively. Figure 2.4 is a simplified block diagram of an ANC system.

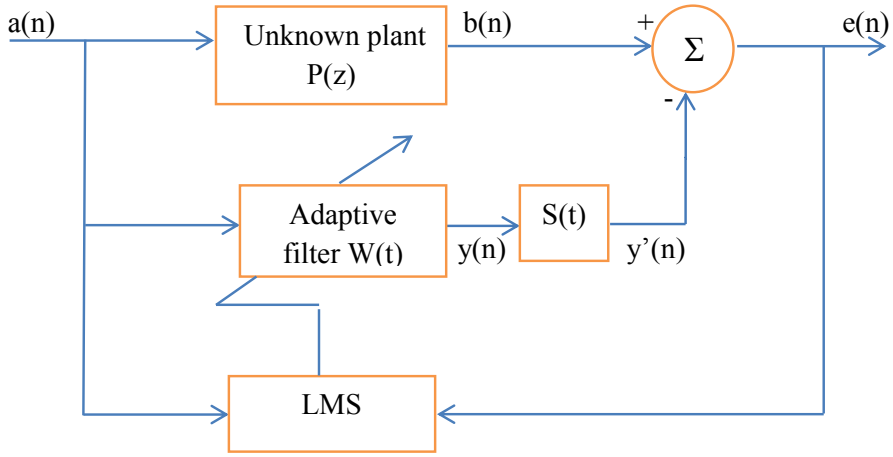

Figure 2.4: Simplified block diagram of an ANC system (Lopez-Caudana *et al.,* 2008)

2.5.1 Feed forward control system

A feed-forward control system is a system in which a prevention of the disturbance is offered, producing an output to counter the disturbance as it arrives. It consists of a reference microphone, an active loudspeaker and an error microphone which measures the level of noise cancellation. This approach works on the principle that the propagation time delay between the input microphone and speaker provides an avenue to electrically reintroduce the noise at a position in the field where it will drive cancellation to occur (Kuo *et al.*, 1998). In addition to this, causality must also be satisfied. Acoustic delay from the reference

microphone to the secondary loudspeaker is proportional to the distance from the reference sensor to the secondary source. An additional acoustic delay between the secondary loudspeaker and the error sensor is common for both primary noise and cancelling signal. Electric delay (ED) refers to the sum of the group delay of the adaptive filter and the total sum delay of the antialiasing filter (Kuo *et al.,* 1998). Since the adaptive filter necessarily has a causal response, then acoustic delay from the reference microphone to the secondary loudspeaker must be greater than ED. This condition is called the causality effect (Kong and Kuo, 1999). In the simple model presented in Figure 2.5, the primary source emits a wave P(t). This wave is detected by a sensor placed at a distance r_s relative to the primary source and a distance r_t relative to the secondary source and fed to the Adaptive controller C. After the detected signal has been adjusted in phase and amplitude, it is emitted by the secondary source to be superimposed on the unwanted noise. The result of this superposition is then observed at an observation point located at a distance r_u relative to the primary source and a distance r_v relative to the secondary source (Figure 2.6).

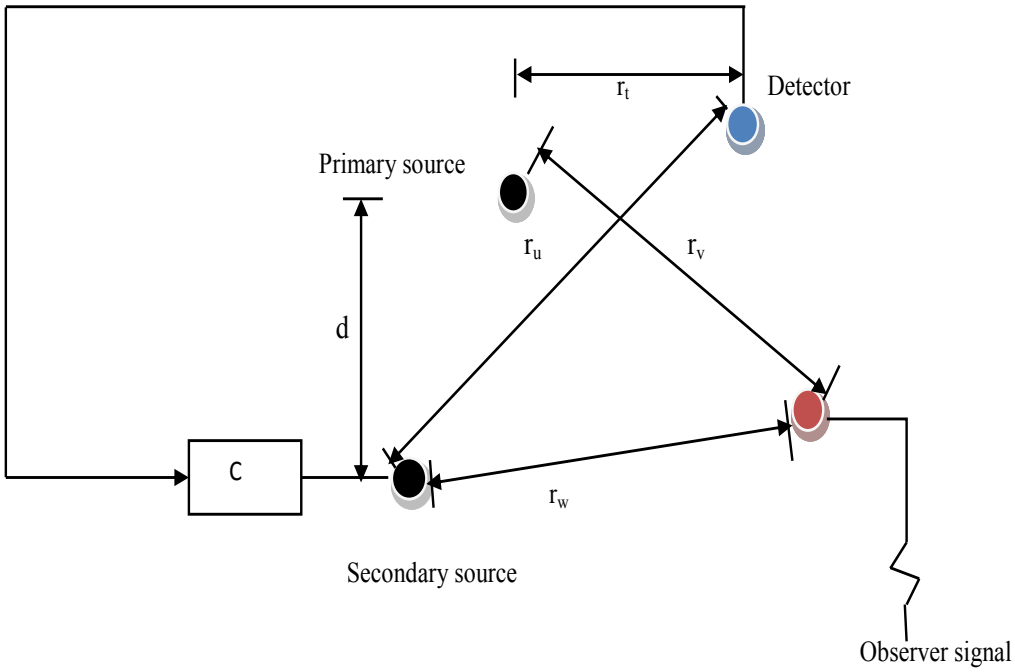

Figure 2.5: Schematic diagram of a feed-forward control system (Swift-Hook, 1989)

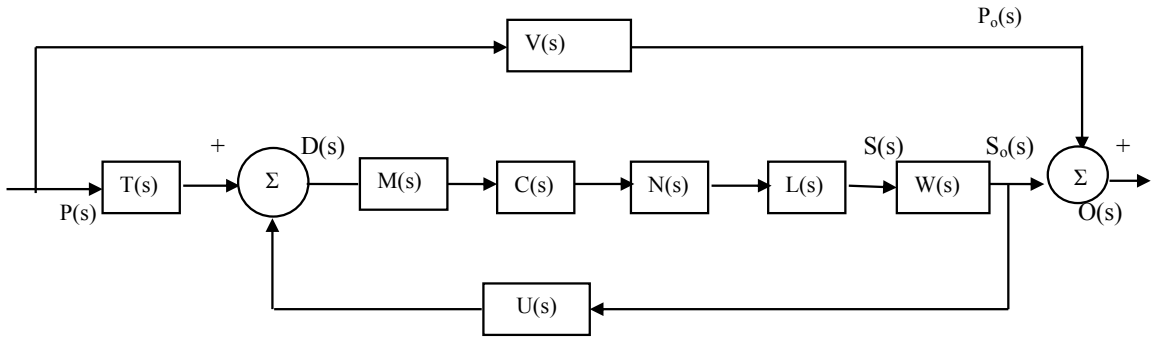

Figure 2.6: A block diagram of feed-forward control system (Swift-Hook, 1989)

From the block diagram, (Figure 2.6):

T(s) Transfer function of path r_t;

U(s) Transfer function of path r_u;

V(s) Transfer function of path r_v;

W(s) Transfer function of path r_w;

M(s) Transfer function of detector;

C(s) Transfer function of the controller;

N(s) Transfer function of necessary electronics;

L(s) Transfer function of the secondary source;

P(s) Primary source output; and

S(s) Secondary source output.

The detector output D(s) and secondary source output S(s) are:

$$D(s) = T(s)P(s) + U(s)S\_0(s) \quad (2.12)$$

and

$$S(s) = M(s)C(s)N(s)L(s)D(s) \quad (2.13)$$

Substituting for (2.12) into (2.13),

$$S(s) = M(s)C(s)N(s)L(s)[T(s)P(s) + U(s)S(s)] \quad (2.14)$$

And the transfer function A(s) between the secondary source and primary source output is given as:

$$A(s) = \frac{S(s)}{P(s)} = \frac{M(s)C(s)N(s)T(s)}{1-M(s)C(s)N(s)L(s)U(s)} \quad (2.15)$$

To cancel noise at the observer position,

$$P_0(s) = -S_0(s) \quad (2.16)$$

From Figure 2.7,

$$P_0(s) = V(s)P(s) \quad (2.17)$$

$$S_0(s) = W(s)S(s)$$

$$S(s) = A(s)P(s) \quad (2.18)$$

Substituting for $P_0(s)$ and $S_0(s)$ from (2.17) into (2.16) using (2.18) gives:

$$V(s) = -W(s)A(s) \quad (2.19)$$

Equation (2.19) is the relation under which full cancellation of noise is achieved at the observation point. Solving for $C(s)$ yields:

$$C(s) = \frac{V(s)}{M(s)N(s)L(s)\Delta(s)} \quad (2.20)$$

where: $\Delta(s) = U(s)V(s) - T(s)W(s)$ (2.21)

A feed-forward control system is an arrangement in which the source of the disturbance is sensed and can be used as a reference for the generation of the control signal (Pathak and Hirave, 2012), and this leads to the removal of the non-zero restriction on the error signal (Hansen and Snyder, 1997). Many of the electronic systems used in feed-forward control systems derive control inputs via modified adaptive signal processing/architecture combinations. Adaptive signal processing is a field born out of the requirements of modern telecommunications systems, where there is a need to filter a signal, so it can be extracted from contaminating noise. In this context, a digital signal processor will be implemented to filter the background surrounding noise from the wind turbine noise. Feed-forward control system is composed of two parts: 'electronic' control system and the 'physical' control system (actuators and sensors) (Hansen and Snyder, 1997). It was further explained that the

feed-forward input carries out the modification of the zeroes of the system in which it is being implemented. The state-space representation of a Single Input-Single Output (SISO) linear dynamical system with 1 input, 1 output and n state variables is:

$$\dot{x}(t) = Ax(t) + Bu(t) + w(t) \tag{2.22}$$

$$y(t) = Cx(t)$$

where:

$A(.)$ is the "state (or system) matrix", $\dim[A(.)] = n \times n$;

$B(.)$ is the "input matrix", $\dim[B(.)] = n \times 1$;

$C(.)$ is the "output matrix", $\dim[C(.)] = 1 \times n$;

$w(.)$ is the "primary disturbance vector" $\dim[w(.)] = n \times 1$; and

$\dot{x}(t) = \frac{d}{dt}x(t)$

$x(.)$ is the "state vector", $x(t) \in \mathbb{R}^n$;

$y(.)$ is the "output vector", $y(t) \in \mathbb{R}^q$;

$u(.)$ is the "input (or control) vector", $u(t) \in \mathbb{R}^p$;

$w(t)$ is equal to m (which is the static gain between input sinusoid $r(t)$ and $w(t)$) given as:

$$w(t) = mr(t) \tag{2.23}$$

If the feed-forward control input's objective is to cancel out the primary disturbance at the error sensor, then it can be shown that:

$$c[mr(t) + Nbr(t)] = 0 \tag{2.24}$$

Substituting for Equation (2.24) into Equation (2.23), and representing the result in frequency domain, output between the output y and reference signal r is:

$$\frac{y(s)}{r(s)} = c(sI - A)^{-1}(Nb + m)r(s) \tag{2.25}$$

From Equation 2.24, it follows that:

$$\frac{y(s)}{r(s)} = 0 \qquad (2.26)$$

This shows that the controller for a feed-forward system places zero transmission at the reference signal frequency.

The feed-forward active noise control structure is able to attenuate both narrowband noise and broadband noise, but the hybrid structure presented by Lopez-Caudana *et al.* (2008), which consists of a feed-forward control system, was implemented to estimate the noise path and a feedback control system used to cancel the feed-back noise

2.5.2 Feedback control

A feedback control system is one that provides reduction of a disturbance by shifting the poles, or natural frequencies of the system (Hansen and Snyder, 1997). Figure 2.7 is a block diagram of a feedback control system and it can be observed that there is no reference sensor. Instead a secondary or cancelling noise is generated by filtering the error signal, which is then sent to the desired noise $d(n)$ to minimize the noise at the error sensor (Mudallah and Mohammed, 2008). This system provides a inadequate reduction over a restricted frequency range for band-limited or periodic noise (Kuo *et al.*, 1996). It can also be instable but has the advantage of not having a feedback of the secondary source output (Behera *et al.*, 2013; Chang and Luoh, 2007).

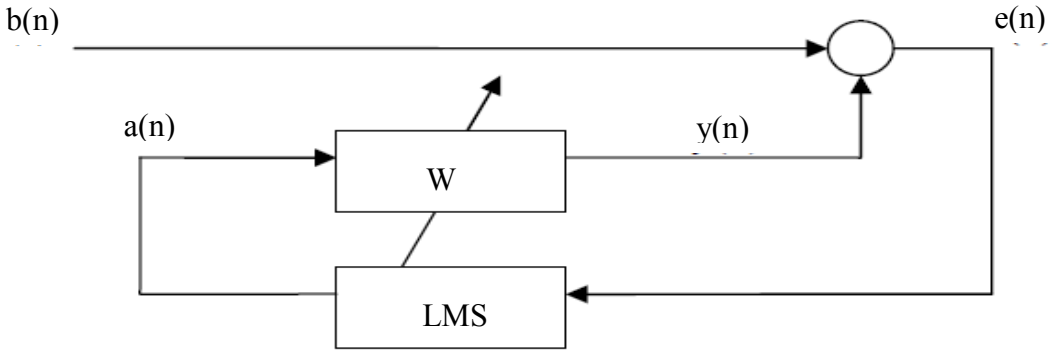

Figure 2.7: Block diagram of a feedback control system

2.6 Adaptive Filters

An adaptive filter is a self-modifying filter that tries to represent the correlation between two signals and it reacts to variations in its parameters in order to bring to bring about a minimal

reduction in the output error (Apolinário, 2009). It is divided into two parts: an adaptive algorithm and a digital filter (Lopez-Caudana *et al.,* 2008). The adaptive filter generally estimates the delay and change in amplitude taking place as the unwanted noise travels from the input microphone to the loudspeaker (Kuo *et al.*, 1996). These delays can be found in electronics, loudspeakers and microphones. Adaptive filters must complete the task of the entire signal processing before the primary noise reaches at the loudspeaker. An adaptive filter modifies itself in such a way that the coefficients are adjusted in order to minimize an error function, which is the measured distance between the reference signal and the output of the adaptive filter. They are estimated to track the ideal behavior of a gradually changing environment. The filter structure, rate of convergence and computational aspects (computational complexity) ought to be taken into account when choosing a suitable algorithm for adaptive filtering (Apolinário, 2009).

2.6.1 Types of errors

Filter coefficient adaptation follows a procedure of minimization of a particular cost function or objective. This function is usually defined as the standard of the error signal $e(k)$. Three common errors used are the instantaneous square error (ISE), the weighted least squares (WLS) and the mean squared error (MSE).

2.6.1.1 The mean-square error

According to Apolinário (2009), the mean squared error could be computed as:

$$\text{MSE}=\xi(n) = E[e^2(n)] = E[|d(n) - y(n)|^2] \quad (2.27)$$

$$\text{If } y(n) = w^T x(n), \quad (2.28)$$

$$\xi = E[|d(n) - y(n)|^2] \quad (2.29)$$

$$E[d^2(n) - 2d(n)w^T x(n) + w^{T^2} x(n)^2] \quad (2.30)$$

$$= E[d^2(n)] - 2w^T E[d(n)\, x(n)] + w^T E[x(n) + x^T(n)]w \quad (2.31)$$

$$= E[d^2(n)] - 2w^T p + w^T R w \quad (2.32)$$

From the above (Apolinário, 2009), p and R are the cross correlation vector and the input signal correlation matrix between the reference signal and the input signal respectively.

They are defined as:

$$R = E[x(n) + x^T(n)] \tag{2.33}$$

$$p = E[d(n)\, x(n)] \tag{2.34}$$

From the above equation, the gradient function of the MSE function with respect to the adaptive filter coefficient vector is given by (Apolinário, 2009):

$$\nabla_w \xi(n) = -2p + 2Rw \tag{2.35}$$

The Wienner solution w_0, that minimizes the MSE cost function, is obtained by equating the gradient vector in the above equation to zero, assuming that R is non-singular:

$$0 = \ -2p + 2Rw_0 \tag{2.36}$$

$$2p = 2Rw_0 \tag{2.37}$$

$$p = Rw_0 \tag{2.38}$$

$$w_0 = R^{-1}p \tag{2.39}$$

Equation (2.39) is the Wienner solution (Apolinário, 2009; Douglas, 1999).

2.6.1.2 The instantaneous square error

Because MSE needs the information of $e(n)$ at every time, it is usually estimated by other cost functions (Apolinário, 2009). Another cost function that can be used is the Instantaneous cost function (ISE), which is given as:

$$\xi_{ISE}(n) = e^2(n) \tag{2.40}$$

In this case, the associated gradient vector with respect to the coefficient vector is given as:

$$\nabla_{\boldsymbol{w}} \xi_{ISE}(n) = 2e(n)\nabla_{\boldsymbol{w}} e(n) \tag{2.41}$$

$$= 2\mathrm{e(n)}\nabla_{\boldsymbol{w}}[d(n) - w^T x(n)] \tag{2.42}$$

$$= -2e(n)x(n) \tag{2.43}$$

2.6.1.3 The weighted least squares error

The weighted least squares (WLS) error is given by (Apolinário, 2009) as:

$$\xi_{WLS}(n) = \sum_{i=0}^{k} \lambda^{k-i}[d(i) - w^T x(i)]^2 \tag{2.44}$$

where $0 \leq \lambda < 1$ is the forgetting factor.

The WLS is based on several samples of error and therefore its stochastic nature reduces in time, being significantly lesser than instantaneous squared error as there is an increase in n.

The ideal linear relationship between the desired and input signals for many cases usually takes the form of a Finite Impulse Response (FIR) (Figure 2.8) or Infinite Impulse Response (IIR) filter (Douglas, 1999; George and Panda, 2013). The FIR filter or Tapped- delay line or Transversal filter is a multiplicative gain within the system (Douglas, 1999). This research will be within the scope of an FIR filter.

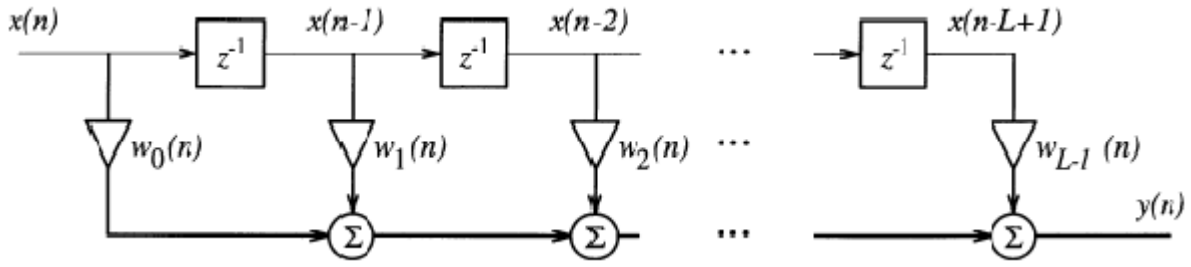

Figure 2.8: Structure of an FIR filter (Douglas, 1999)

The combination of gradient descent algorithm, particularly the Least Mean Square (LMS) algorithm and an FIR filter, form probably the most commonly implemented adaptive filtering system (Pathak and Hirave, 2012). The system is of a simple and robust type, while being effective and having a reasonably fast convergence to a near-optimal solution for all purposes (Apolinário, 2009).

For an FIR structure, $y(n)$ as given as (Douglas 1999):

$$y(n) = w_0 x(n) + w_1 x(n-1) + w_2 x(n-2) + \cdots + w_N (n-N) \quad (2.45)$$

$$\sum_{i=0}^{N} w_i \, x(n-i) \quad (2.46)$$

$$w^T x(n) \quad (2.47)$$

where N is the filter order and $\boldsymbol{x}(n)$ and w are vectors composed of the input-signals samples and the filter coefficients.

$$x(n) = [x(n), x(n-1), x(n-2), \ldots, x(n-N)]^T \quad (2.48)$$

$$w = [\, w_{0,} \, w_1, w_2, \ldots, w_N]^T \quad (2.49)$$

For complex implementation;

$$y(n) = w^H x(n), \tag{2.50}$$

where superscript H denotes the Hermitian operator (Douglas 1999).

The general form of an Adaptive filtering algorithm is expressed as:

$$W(n+1) = W(n) + \mu(n)G(e(n), \phi(n)) \tag{2.51}$$

where:

G(.) Particular vector-valued nonlinear function;

$\mu(n)$ Step size parameter;

$e(n)$ and $X(n)$ are the error signal and input signal vectors, respectively; and

$\phi(n)$ Vector of states that stores pertinent information about the characteristics of the input and error signals and the coefficients at previous time instants (Douglas, 1999).

2.7 FXLMS Algorithm

The LMS algorithm is the basic algorithm applied to adaptive filters. Most recent algorithms today find its roots from the LMS algorithm (Pathak and Hirave, 2012). One of the reasons for the popularity of LMS algorithm is owing to the fact that there is a similarity between the type and number of operations needed for the algorithm and the FIR filter structure having fixed coefficient values (Douglas, 1999). The performance of an ANC system however, becomes unstable if the LMS algorithm is used without modification (Zhu, 2009; George and Panda, 2013), which occurs when there is a misalignment in time with the reference signal, due to the existence of secondary path transfer function $S(t)$ (Kuo, 1999; Erkan, 2009). To ensure that the system converges, the input to the error correlation is filtered by a secondary path estimate $\hat{S}(z)$ (Pathak and Hirave, 2012). Hence, the filtered-x-least mean squared (FxLMS) algorithm.

The most common algorithm used in ANC is the FXLMS (Sun *et al.*, 2006) algorithm as shown in Figure 2.9. This is because through it, transfer function in real time can be obtained and it gives opportunity for changes in noise characteristics and the environment of the system, which leads to maintenance of the convergence performance (Yang *et al.,* 2013). It

minimizes the residual error $e(n)$ by adjusting the adaptive filter W followed by the secondary path S (Krystajic *et al.,* 2013). FXLMS was developed by using an adaptive filter as the controller (George and Panda, 2013), and the output of the controller in time n is given by:

$$y(n) = aT(n)\, a(n) \tag{2.52}$$

Where: $a(n)=\begin{bmatrix} a_1(n) \\ a_2(n) \\ \vdots \\ a_{N_2}(n) \end{bmatrix}^T$ is the weight vector of the controller and

$a(n) = \begin{bmatrix} a(n) \\ a(n-1) \\ \vdots \\ a(n-N_1+1) \end{bmatrix}^T$ is the tap delayed signal vector. The residual noise is given by

$$e(n) = b(n) - s(n) * y(n) \tag{2.53}$$

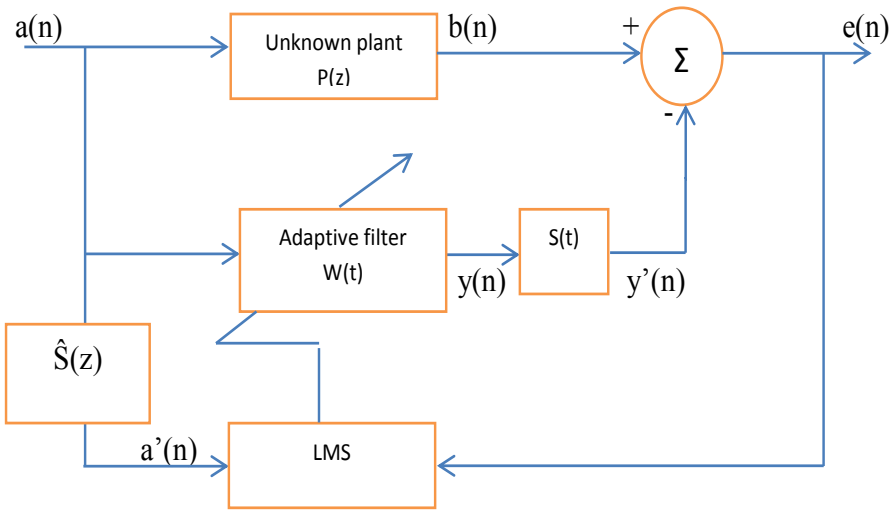

Figure 2.9: Block diagram of an FxLMS ANC system (Akhtar *et al.*, 2005)

From Figure 2.9:

$$e(n) = b(n) - y'(n) \tag{2.54}$$

Substituting for $y'(n) = S(n) * y(n)$ into (2.54),

$$e(n) = b(n) - s(n) * y(n) \tag{2.55}$$

$$e(n) = d(n) - s(n) * [w^t(n)a(n)] \quad (2.56)$$

where * is the linear convolute operator and $s(n)$ is the impulse response of the secondary path; and

$$s(n) * y(n) = \sum_{i=\infty}^{\infty} s(i)y(n-i) \quad (2.57)$$

The adaptive filter and the LMS algorithm have the same aim, and it is to minimize the instantaneous squared error.

$$\check{E}(n) = e^2(n) \quad (2.58)$$

Applying the method of gradient descent, but changing ξ(n) for $\check{E}$(n);

$$w(n+1) = w(n) - \frac{\mu}{2}\nabla\check{E}(n) \quad (2.59)$$

$$\nabla\check{E}(n) = \nabla e^2(n) = 2[\nabla e(n)]e(n) \quad (2.60)$$

If $\nabla e(n)$ = -S(n)*a(n) ≙ -x' (n), then:

$$\nabla\check{E}(n) = \nabla e(n)2e(n) \quad (2.61)$$

$$\nabla\check{E}(n) = -2\, a'(n)\, e(n) \quad (2.62)$$

Substituting Equation (2.62) back into Equation (2.59):

$$w(n+1) = w(n) + \mu\, a'(n)e(n) \quad (2.63)$$

Equation (2.63) is the derived FXLMS algorithm.

where: μ is the step size of the algorithm which determines the stability and convergence of the algorithms and $a'(n)$ the filtered version of reference input.

When this algorithm is executed, filter convergence can be achieved much more faster than theory suggests (Sen *et al.,* 1996). The maximum value of step size μ ensuring convergence is:

$$\mu_{max} = {}^{1}/_{Px'}(L + \Delta) \quad (2.64)$$

where:

Px' is the power of the filtered reference signal; and

L and Δ are the amounts of the delay in the secondary path.

$$Px^{'} = E\left\{\left(x^{'}(n)\right)^{2}\right\} \quad (2.65)$$

2.8 Summary

In this literature review, a brief summary of the behavior of sound waves and how they are radiated from wind turbines is presented. Passive methods that have been used are also studied. Conclusions have been made on the fact that these passive methods work well in reducing high frequency noise but are inefficient in reducing the low frequency noise from wind turbines. Active noise control however works well in reducing low frequency noise. Past studies that have implemented ANC are studied and the importance of a proper control system has also been explained.

The present study focuses on feed-forward ANC whilst using an FIR adaptive filter structure for wind turbine noise reduction. A single-input single-output system will be implemented. All these will be carried out to investigate the residual noise.

CHAPTER THREE
PROBLEM ANALYSIS

3.1 Introduction

Due to increase in both structural size and power output, the challenges of wind turbine noise in wind technology has also increasingly become an issue of great concern to humans and animals habiting in close proximity to wind farms where wind turbines are installed. This has been considered as one of the negative impacts of wind turbine technology. The blades in a typical wind turbine while rotating drives the gear train which produces both gear train noise and aerodynamic noise caused by the blade passage through the air and resulting in vortices being shed from the edges of the blade. This chapter provides good and in-depth knowledge of the sources of noise as a problem, its implications and analysis. This is necessary in order to identify ways to reducing or outright elimination of them. Wind turbine noise is not initially considered impulsive due to its less constant level; however they can produce impulsive sounds in specific atmospheric conditions. This goes to explain that the atmospheric or weather condition at a particular time can directly influence the type of sound produced by wind turbine blades. From the previous section, it has been established that wind turbine noise can be broadly classified into mechanical and aerodynamic noise. This present section elaborates more on these different noise sources and the mechanisms of their production. Figure 3.1 is a schematic flow chat of the various classifications of wind turbine noise especially as they relate to the subject of this study.

3.2 Mechanical Noise from Wind Turbines

Mechanical noise from wind turbines occurs as a result of vibration between equipment and materials. Frictions and contacts with engine components such as gearbox, generator, and yaw drives can be the main cause(s) of mechanical noise. Situations like misalignment, misbalancing, coupling inaccuracies, bent rotor shafts and lack of lubricating oils (friction) can induce such noises (Norton and Karczub, 2003). The noise emanating from gears is as a result of gear teeth interaction. Even when these perceived fault(s) are not evident; the dynamic forces generate impulsive and broadband noise (Norton and Karczub, 2003). The impulsive noise is related to the various meshing impact process while the broadband noise is

associated with friction, fluid flow and general gear system structural vibration and noise radiation (Norton and Karczub, 2003). Gear geometry factors and variations of load and speed also contribute to gear noise (Norton and Karczub, 2003).

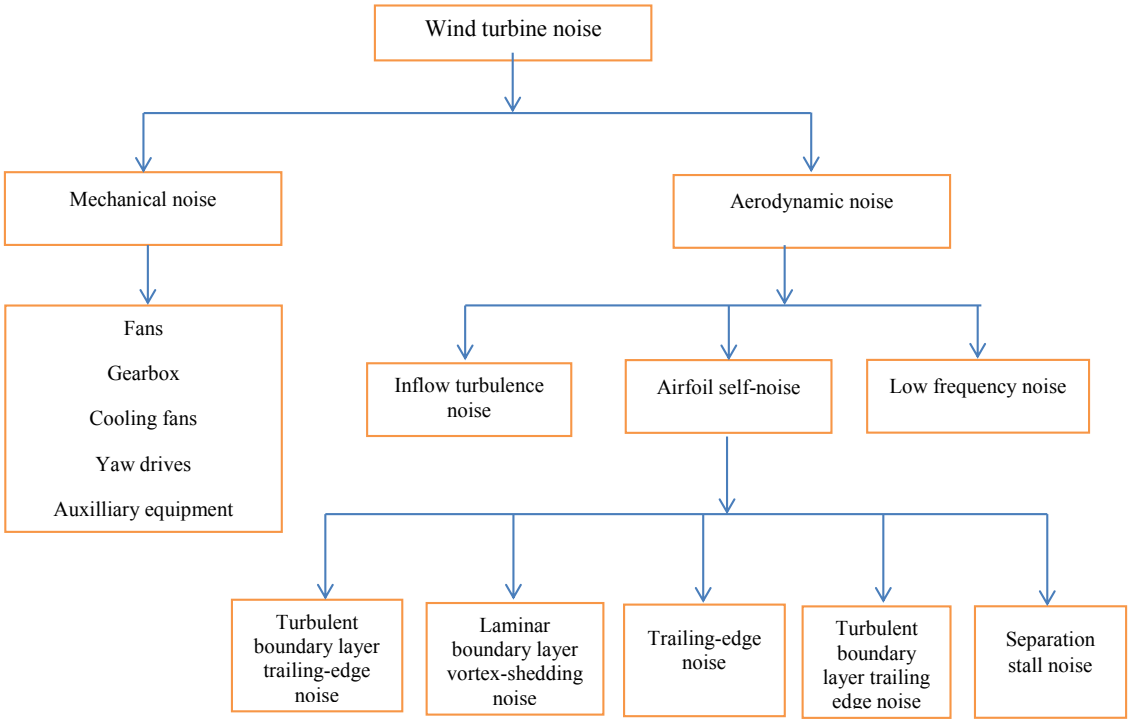

Figure 3.1: Classification of noise in a wind turbine

In rotors and shafts, misalignment and misbalancing are the common faults associated. The vibrations for misalignment are both radial and axial, while with misbalancing, the vibration is generally radial and the increase in noise and vibration is at the rotational frequency (Norton and Karczub, 2003). So far, mechanical noise from wind turbines has been taken care of with new technologies of designs and no longer poses a serious problem because wind turbines are now being designed to also accommodate mechanical noise(s). These, according to Migliore and Oerlemans (2003) are:

- Low speed cooling fans;
- Special finishing of gear teeth;
- Mounting components in the nacelle;
- Using damping methods to reduce vibrations within the tower;
- Adding insulations to the nacelles; and

- Using damping methods to reduce the vibrations inside the hub.

Figure 3.1 depicts the various classifications of noise from wind turbines. According to this classification, wind turbine noises are either from the interaction of the blade with air or from mechanical components in the nacelle or tower.

3.3 Aerodynamic Noise from Wind Turbines

Aerodynamic noise is produced from the flow of air over the rotating blades. This type of noise can be broadband in nature and caused by turbulence. As a wind turbine blade in operation slashes through the air, it forces air movement from left to right. The effective flow speed V is comprised of the wind speed V_w and the rotational flow speed V_r (Oerlemans, 2011). When determining flow features and quantifying airfoil performance such as lift and drag, the transition from laminar to boundary layer plays a major role (Eleni *et al.*, 2012). When a rotating wind turbine blade encounters air flow, due to viscosity, it develops a thin layer of air which 'adheres' to the blade surface and this layer can be termed the boundary layer (Oerlemans, 2011). Aerodynamic noise is classified into Inflow turbulence noise, airfoil self-noise and low frequency noise.

The interaction between the incidents eddies and the surface of the blade may lead to what is called the inflow turbulence noise, while airfoil self-noise is as a result of the interaction of the airfoil and air. It is produced from an undisturbed inflow and is highly dependent on the pressure difference between the pressure and suction side of the blade and the blade tip (Oerlemans, 2011). Low frequency noise on the other hand is noise in the frequency range of 20-500Hz.

3.3.1 Inflow turbulence noise

This is a form of aerodynamic low-frequency noise that arises when an airfoil encounters an unsteady flow owing to wakes from an upstream turbine (Lloyd *et al.,* 2012). Recent study of Lee *et al.* (2013) indicates that this noise level depends on the inflow velocity and the characteristics of turbulence while a more recent work of Larato *et al.* (2014) gives information that large amounts of this type of noise produces noise at far distances due to their low frequency nature (Larato *et al.*, 2014).

Inflow turbulence (IT) noise is as a result of the interaction between the leading edge of the airfoil and a turbulent inflow (Moriarty and Migliore, 2003). This can also be called leading edge noise and it depends on the angle of attack, flow speed, shape of the airfoil and radiation direction (Oerlemans *et al.*, 2009). Due to its significant importance, lots of research incursion have gone into simulation, prediction and modelling in order to evaluate the different phenomena associated with it (Tian *et al*., 2013; Lloyd *et al*., 2012; Moriarty and Migliore, 2003; Leloudas *et al.*, 2007). Some of these research outputs include a proposal made by Tian *et al.* (2013) which comprised of a theoretical noise prediction model that may possibly be utilized for studying different occurrences of wind turbine noise. It was concluded that increase in airfoil resulted in a corresponding reduction in inflow turbulence noise. The importance of IT noise is dependent on the structure of the atmospheric turbulence and on the shape of the blades and is triggered by the collaboration of upstream turbulence with the blades which also depend on the atmospheric circumstances. IT noise has been studied numerically using synthetic turbulence and Improved Delayed Detached-Eddy Simulation (IDDES). The IDDES extension reformulates the length scales so as to resolve part of the boundary layer in unsteady mode (Lloyd *et al*., 2012). This category of noise is a significant basis of low frequency noise on wind turbines, which is produced when the rotating blade comes across deficient flow in close proximity to the tower, wakes and sheds from the other blades and wind speed changes (Rogers and Manwell, 2004).

Studies by Van den Berg (2004) suggested that a key input to the low frequency sound may be the outcome of sudden variation in airflow the blade comes in contact with when it passes the tower; however, he explains that this effect has not probably been perceived as significant as the blade passing frequency is considered to be insensitive. The studies also indicate that although infrasound levels from large wind turbines at 20Hz are low and inaudible, they might cause structural elements of buildings to vibrate (Berglund *et al.*, 1996) on the other hand even though low frequency inflow turbulence may be capable of being heard by the human ear, it is however loudest at medium to high frequency. Turbulent inflow becomes essential when the length scale of the turbulent eddies is great as compared to the leading edge radius of an airfoil (Moriarty and Migliore, 2003). Studies carried out by Tian *et al*. (2013) proposed an improvement on the adaptation of the analytical model by Amiets theory. One of these proposals was an empirical airfoil thickness correction in the turbulent inflow noise model which included Doppler effects for rotating blades. The model for turbulent inflow noise by Amiet (1975) is given as:

$$L_{p=}10\log\left[\rho_{0^2}c_{0^2}\mathcal{L}\frac{\Delta L}{r^2}M^3I^2\acute{k}^3\left(1+\acute{k}^2\right)^{-7/3}\right]+58.4+10log\left[\frac{K_c}{1+K_c}\right] \qquad (3.1)$$

where:

$\mathcal{L}$ Turbulence length scale [-];

I Turbulence intensity [-];

ρ_0 Density [kg/m^3];

c_0 Speed of sound [m/s];

ΔL Blade segment semi-span [m];

$\acute{k}$ Corrected wavelength [-]; and

K_c Low frequency correction [-].

The dimension of the turbulence length scale ($\mathcal{L}$) and the square of the turbulence intensity (I^2) are essential in the investigation of IT noise. For wind turbines (WT), the inflow turbulence may be due to atmospheric boundary layer turbulence or wakes from upstream turbine (Lloyd *et al*., 2012; Oerlemans, 2011). The properties of the incoming turbulence are highly reliant on the characteristics of inflow. Because the frequency of the radiated sound is given as: $f \sim {}^{U}/_{\Lambda}$, the spectrum of inflow turbulence noise is related directly to the spectrum of the incoming turbulence and atmospheric turbulence which is of a natural nature, is expected to cause broadband noise for frequencies up to 1000Hz (Oerlemans, 2011).

3.3.2 Airfoil self-noise

In airfoil self-noise, the noise generated has no direct influence from atmospheric turbulence (Lee *et al*., 2013) and is therefore produced via a smooth, non-turbulent in-flow. Airfoil self-noise is generated from the interaction between the turbulent flow over airfoil and the blades trailing edge or turbulence produced in its own boundary layer and near wake when encountering a non-turbulent inflow (Oerlemans, 2011; Moriarty and Migliore, 2003). It takes place in the outboard region of wind turbine blades (Lee *et al.,* 2013) and can be divided into turbulent boundary layer trailing edge noise, separated flow noise, laminar boundary layer vortex shedding noise, tip vortex formation noise and tower wake interaction noise. Because empirical modelling of the individual noises cannot be carried out directly,

semi empirical methods have been formulated based on measurements and is capable of predicting individual sources of aerodynamic noise with precision.

3.3.2.1 Turbulent boundary layer trailing edge noise

Turbulent boundary layer trailing edge noise originates from the contact between the boundary layer and the trailing edge of the airfoil (Jianu *et al.,* 2012) and it defines the lower bound of wind turbine noise. Brooks and Hodgson (1981) presented a diagram of an airfoil in uniform flow generating noise from the interaction of turbulent boundary layer and a trailing edge as shown in Figure 3.2. The intensity of the noise is proportional to the turbulent boundary layer displacement thickness and the fifth power of the Mach number and inversely proportional to the square of the distance between the observer and the airfoil trailing edge (Moriarty and Migliore, 2003). The sound pressure level as given by Moriarty and Migliore (2003) is:

$$SPL_{pressure} = 10log\left[\frac{\delta^{*}{}_{pressure}M^{5}L\dot{D}_{func}}{{r_e}^{2}}\right] + A\left[\frac{St_{pressure}}{St_1}\right] + (k_1 - 3) + \Delta K_1 \qquad (3.2)$$

where:

$SPL_{pressure}$ is the sound pressure level of the turbulent boundary layer trailing edge noise

δ^{*} Boundary layer displacement thickness for the pressure side [m];

M Mach number [-];

r_e Distance between observer and airfoil trailing edge [m];

L Span of the airfoil [m];

$\dot{D}_{func}$ Directivity function [-]; and

A An empirical spectral shape based on the Strouhal number, St [-].

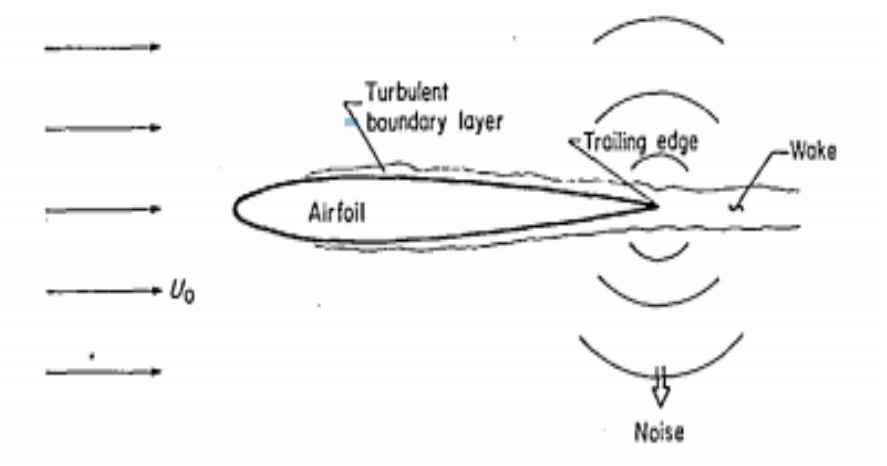

Figure 3.2: Airfoil in uniform flow encountering noise from turbulent boundary layer trailing edge Source: Brooks and Hodgson (1981).

3.3.2.2 Laminar boundary layer vortex shedding noise

Laminar boundary layer vortex shedding noise is generated as a result of a feedback loop caused by vortices being shed at the trailing edge and unsteady waves in the laminar boundary layer upstream of the trailing edge (Moriarty and Migliore, 2003). It has been said to occur when a laminar boundary layer exists over most of at least one side of an airfoil. The vortex shedding is apparently coupled to acoustically excited aerodynamics feedback loops (Göçmen and Ozerdem, 2012; Brooks *et al.,* 1989). Figure 3.3 shows an airfoil encountering laminar boundary layer vortex shedding noise (Brooks *et al.*, 1989). Pressure waves are propagated upstream and amplify instabilities in the boundary layer as a laminar vortex leaves the trailing edge (Brooks *et al.*, 1989) and it occurs on small wind turbines at Reynolds number smaller than 1 million and emits a type of "whistling" noise (Oerlemans, 2011). According to the work carried out by Moriarty and Migliore (2003), the empirical relation for sound pressure level of laminar boundary layer vortex shedding noise is given as:

$$SPL_l = 10log\left[\frac{\delta_p M^5 L\dot{D}_{func}}{{r_e}^2}\right] + G_1\left[\frac{St'}{St'_p}\right] + G_2\left(\frac{Re_c}{(Re_c)_0}\right) + G_3(\alpha) \qquad (3.3)$$

where:

SPL_l Sound pressure level of the laminar boundary layer vortex shedding noise [dB];

δ_p Boundary layer thickness for the pressure side [m];

M Mach number [];

r_e Distance between observer and airfoil trailing edge [m];

L Span of the airfoil [m];

$\dot{D}_{func}$ Directivity function [-];

G_1 G_2 and G_3 are empirical functions [-];

St' Strouhal number based on δ_p [-];

St'_p Peak Strouhal number [-]; and

$(Re_c)_0$ Reference Reynolds number [-].

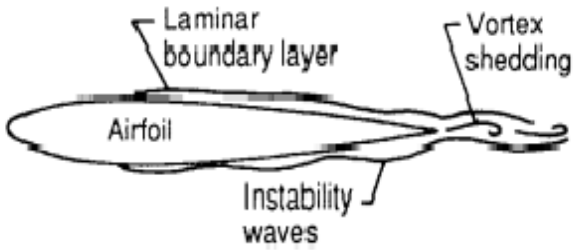

Figure 3.3: Airfoil in uniform flow encountering laminar boundary layer vortex shedding noise Source: Brooks et al. (1989).

3.3.2.3 Trailing-edge bluntness vortex shedding noise

When there is vortex shedding from a blunt trailing edge, noise is produced and this is referred to as trailing-edge bluntness vortex shedding noise; its geometry is determined by the frequency and amplitude of the trailing edge (Moriarty and Migliore, 2003). According to Oerlemans (2011), this type of airfoil self-noise is said to occur when the thickness of the trailing edge is increased over a critical value and they can be prevented by designing blades properly. A study from Moriarty and Migliore (2003) explains that the predicted sound pressure level of this noise is given as:

$$SPL_T = 10log\left[\frac{\delta_p{}^* M^5 L \dot{D}_h}{{r_e}^2}\right] + G_4\left(\frac{h}{\delta^* avg}, \Psi\right) + G_5\left[\frac{h}{\delta^* avg}, \Psi, \frac{St^{"}}{St^{"}{}_{peak}}\right] \quad (3.4)$$

where:

SPL_T Sound pressure level of the trailing-edge bluntness vortex shedding noise [dB];

h Trailing edge thickness [m];

δ^*_{avg} Average displacement for both sides of the airfoil [m];

Ψ Angle between both airfoil surfaces [deg];

St'' Strouhal number based on h [-];

St''_{peak} Peak Strouhal number [-];

G_4 and G_5 are empirical functions of the parameters [-].

M Mach number [-];

r_e Distance between observer and airfoil trailing edge [m];

L Span of the airfoil [m]; and

$\dot{D}_h$ Directivity function [-].

The diagram of an airfoil encountering trailing-edge bluntness vortex shedding noise is given by Brooks *et al*. (1989) in Figure 3.4.

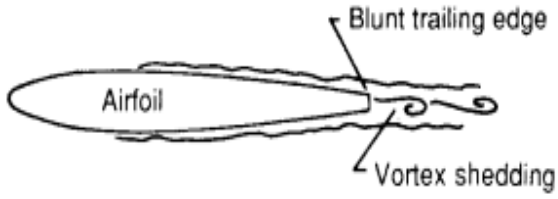

Figure 3.4: Tailing-edge bluntness vortex shedding noise Source: Brooks et al. (1989).

3.3.2.4 Tip vortex formation noise

Tip vortex formation noise is as a result of interaction between the blade tip and the trailing edge of the airfoil. This noise is three-dimensional in nature (Moriarty and Migliore, 2003). It has been said to originate from pressure difference between the pressure side and suction side of the wind turbine blades (Oerlemans, 2011). Tip noise should be accorded more study and research as there are still more to be understood with regards to the mechanism of the noise generation. (Arakawa *et al.*, 2005). A diagram of the mechanism of formation is shown in Figure 3.5.

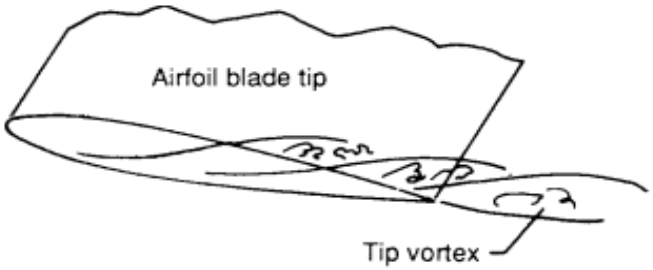

Figure 3.5: Tip vortex formation noise. Source: Brooks et al. (1989).

3.3.2.5 Separation-stall noise

Increase in the angle of attack leads to a corresponding separation of flow from the suction side of the wind turbine blade airfoil (Oerlemans, 2011). This separation from the suction side in turn increases the level of sound emission through growth in size of the boundary layer and vortex shedding (Laratro *et al.*, 2014). The study of separation-stall noise is of importance because wind turbine airfoils operate at high angle-of-attacks for a long time (Jianu *et al.*, 2012). According to studies by Laratro *et al.* (2012), the flow field in the wake of a horizontal axis wind turbine (HAWT) is not well established and therefore true angle-of-attack distributions have not been produced. Figure 3.6 shows separation-stall noise in which the separated boundary layer becomes turbulent and interacts with blade surface.

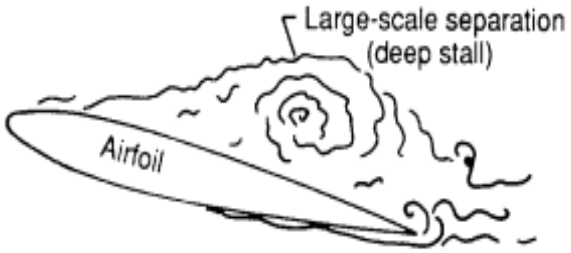

Figure 3.6: Separation-stall noise. Source: Brooks et al. (1989).

3.3.3 Low Frequency noise and infrasound from wind turbines

Low frequency noise spans the infrasonic and audible ranges and may be well thought-out as the range from about 10 - 200Hz (Bengtsson, 2004), but with range 10 - 100Hz of most interest (Leventhall, 2003) and are produced by both rotating and reciprocating machineries. Since atmospheric absorption attenuates high frequencies at a higher rate with distance than lower frequencies, low frequency noise propagates farther and leaves negative effects on

individuals residing close to the source. Wind atmospheric turbulence which is of a natural source is expected to cause broadband noise for frequencies up to 1000Hz (Oerlemans, 2011). A wide study of various reviews on Low Frequency Noise and its effects have been carried out by Leventhall (2003), which has shown that low frequency noise is correlated with annoyance. It was also established that low frequency noise resulted in wakefulness and a decline in daily task performance. Past attempts to reduce noise from wind turbines have not been giving consideration due to the fact that noise from wind turbines blades are broadband; therefore it consists of low and high frequencies and different approaches are to be followed in reducing or eliminating them. Extensive research have also been carried out on noise reduction using passive methods (Göçmen and Özerdem, 2012; Rogers and Manwell, 2004; Scheppers *et al.,* 2007; Oerlemans *et al.,* 2009; Leloudas *et al*., 2007; Howe, 1991 and Geyer 2010) which were able to reduce high frequency noise components.

Low Frequency (LF) Noise can be described as sounds which are unwanted and containing major constituents within specified frequency range (Berglund *et al.,* 1996). This has to do with the low frequency part of the sound spectrum, LF noise from wind turbine blades are generated when rotating blades encounter localized flow deficiencies due to the flow around a tower, wakes and shed. These localized deficiencies could originate from other blades and changes in wind speed. This is also referred to as tip noise and can as well be produced by pressure fluctuations and loading distributions around the blade (Son *et al.,* 2010). The effects of low frequency noise are of precise concern not only because of the health and environmental impacts but also on the effect it has on the overall efficiency of wind turbines.

A, B, C and G-weighting refers to the different sensitivity scales for noise measurements. A-weighting shapes the spectrum according to the sensitivity of human hearing, which leads to a complete underestimation of the likely influence of infrasonic and low-frequency noise in the ear (Salt and Hullar, 2010); the use of A-weighting was said to be a problem when detecting the frequency spectrum of infrasound and Low-frequency noise from wind turbines because infrasound should therefore be measured using G-weighting curve as this weighting scales can pick frequencies as low as 20Hz.

3.3.3.1 Sources and transmission of low frequency noise from wind turbines

Apart from the turbine blades, low-frequency loading noise can also be generated from the wind turbine rotor, which is as a result of steady loading being applied to the blades while rotating (Lee and Lee, 2014). The lower frequencies are of infrasound nature and it has both

broadband and amplitude modulated pattern in rhythm with the blade passing frequencies (Jakobsen, 2005) which may be made audibly by interference patterns and other propagation effects (Laratro *et al*., 2014). This occurs as a result of fluctuating aerodynamic loading and it is one of the main noise sources of rotating machineries, such as helicopter rotors, turbo-machinery, and fans (Jakobsen, 2005). In a study to examine the aerodynamic noise which was produced by small wind turbines, numerical predictions and measurement indicated that low frequency broadband noise was generated when atmospheric turbulence is ingested into the wind turbine rotor (turbulence ingestion noise) (Lee and Lee, 2014).

A parametric investigation on the estimation and control of aerodynamic noise from wind turbines has been studied and it was concluded that the blade tower interaction is the main source of low frequency noise (Laratro *et al*., 2014) and this is shown in Figure 3.7. In this mechanism of noise generation, the rotating blades come across contained flow deficits as a result of the tower wake (Errasquin, 2009).

Cyclostational spectral analysis was employed to predict and analyze aerodynamic noise generated by wind turbines and it was ascertained that swishing is the result of an amplitude modulation of the broadband aerodynamic noise which occurs at the blade passing frequency (Cheong and Joseph, 2014).

3.3.3.2 Problems and the negative impacts of low frequency wind turbine noise

Low frequency noise in wind turbines have obviously received less concern, however they mask higher frequencies, cross greater distances and has the ability to bring about resonance in human body (Berglund, 1996). Contrary to belief that infrasonic noise and some low-frequency noise are inaudible (Jakobsen, 2005; Berglund *et al.,* 1996), it has been established that hearing does not stop at 20Hz, as humans can hear infrasound as little as up to 1Hz (Møller and Pederson, 2011). Infrasonic and low-frequency sounds which are perceived as inaudible can influence the function of the human ear as it is likely to have more effect on the structures of the inner ear (Salt and Hullar, 2010).

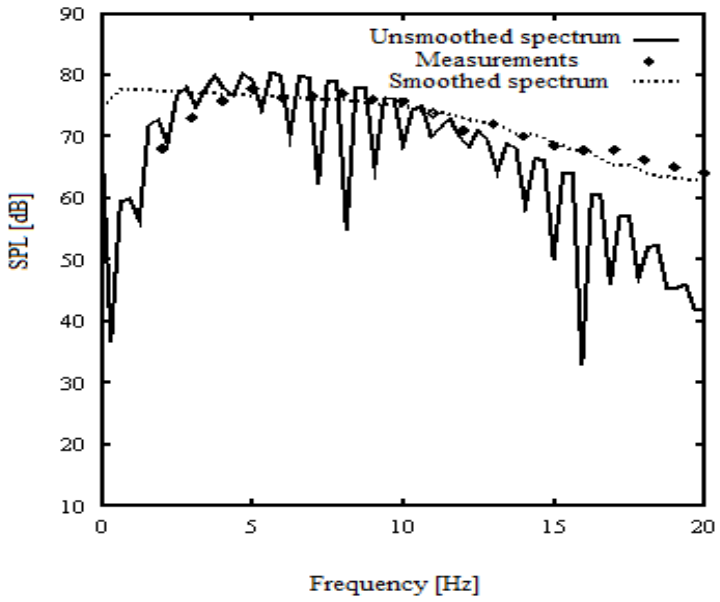

Figure 3.7: Blade tower interaction noise spectrum Source: Errasquin (2009).

Schust (2004) reviewed the consequence of low frequency noise up to 100Hz on some physiological parameters, performance and subjective complaints, which was validated by carrying out laboratory experiments and field studies related to the threshold of hearing. It was concluded that there was no systematic confirmation for a connotation between A-frequency weighted sound pressure level and the biological effect, there was also no substantial differences in medical or psycho-social symptoms (Waye and Rylander, 2001). There was a distinct dependence on frequency of the hearing threshold in the low frequency range with a steep slope when likened to the middle frequency range.

The consequences of exposure to moderate levels of low-frequency noise and a flat-frequency noise was studied by Bengtsson *et al*. (2004) in which a comparison was made to determine whether low frequency noise could result in performance impairment during work. The tasks carried out were picked to be sensitive to exhaustion and enthusiasm. Pearson's correlation analysis (Bengtsson *et al*., 2004) was implemented to ascertain relationships between the following: performance results, subjective reports and subjective sensitivity while also analyzing the correlation between cortisol levels and the stress and energy reported. At the end of the study, a connection was found between motivation and concentration for the noise conditions studied. Noise irritation as a result of low frequency was the positively correlated to the absence of attentiveness, fatigue and eardrum pressure

which leads to overall rise in annoyance, while these relationships were not found for the flat-frequency noise condition. A conclusion was reached that low frequency noise had an undesirable effect on monotonous and routine type character which resulted in tiredness and routine type character.

A study by Di *et al.* (2011) investigates the influence of adding another sound to low frequency noise. Paired comparison test was used to evaluate the combination of low frequency noise with frequency modulated pure tones, pink noise and natural sounds. The Bradley-Terry model was used to obtain the subjective annoyance value (SAV). The psychoacoustic annoyance value (PAV) was also calculated and its correlation alongside SAV analyzed. When pink noise of 250-1000Hz was added to the low frequency noise, the subjective annoyance declined, and then ascended linearly. When natural sound and FM sounds was added, the SAV increases with increasing sound pressure level of the combined sound. The studies suggested that there was an acceptable relationship between the subjective annoyance value and the variation extent of frequency modulated pure tones.

The amplitude modulation (AM) frequency of a 31.5Hz tone and the stability of high and low frequencies in a low frequency noise were interactively varied with the sole purpose of generating a more pleasing or less unpleasing low frequency noise using subjects who were allowed to adjust the low frequency noise (LFN) to their desired levels (Bengtsson, 2004). The results advocated that a higher or lower frequency modulation as opposed to the original LFN. The combination of a low frequency noise with both an agreeable frequency balance was regarded as less required to be changed and not so annoying.

The results of the study carried out on mental performance by Pawlaczyk-Luszyczyniska *et al*. (2005), indicates that low-frequency noise at reasonable levels might severely affect visual functions, concentration, continuous and selective attention.

Apart from the effect on humans, they may also lead to vibrations in structural elements of buildings (Berglund *et al*., 1996; Van den Berg, 2004). The World Health Organization (WHO) identifies the distinct place of low frequency noise as a cause of environmental noise pollution and the annoyance associated with it stems from acoustical signals (Leventhall, 2004).

3.3.3.3 Low frequency noise reduction procedure

Results from studies conducted by Tian *et al.* (2013) shows that increase in airfoil leads to a reduction in turbulent inflow noise, however, the thickness correction did not seem significant when the atmospheric turbulent length scale was very large. Passive control methods also rely heavily on structural resonance; membranes and plates have been used in many cases and their main effects have been the mass required to achieve such resonance (Wang and Huang, 2009). Active noise control should be well-thought-out as a feasible option since less space is needed for its installation and it is most efficient at low frequencies (Romeu *et al*., 2014). Modern active noise control is accomplished using analog circuits or digital signal processing. The waveform of the background noise are analyzed using adaptive algorithms which in turn generate another signal that either shift the phase or invert the polarity of the source signal This phase-shifted source signal is then amplified and a loudspeaker (transducer) creates a sound wave which is in direct proportion to the original waveforms amplitude, and resulting in destructive interference. The current research seeks to investigate the feasibility of using active noise control in reducing the low frequency noise from wind turbines. It should be noted that since passive methods have worked well in attenuating the high frequency components of noise from wind turbines, then both active and passive methods should be used together as they complement one another.

3.4 Summary

In this Chapter, the analysis of wind turbine noise is presented and their root cause or sources from different approaches have been implemented. The sources of mechanical and aerodynamic noise have been studied and it has been shown that mechanical noise is no longer an issue for modern wind turbines as current designs have very minimal mechanical noise due to the implementation of various vibration controls and proper padding methods. However, aerodynamic noise is still an issue that is still receiving active research. Some of these aerodynamic noises are low frequency in nature and are the main sources of annoyance. This has led to a need for more critical analysis of low frequency aerodynamic noise. Since active noise control works well for low frequency noise, it will be used as it requires less space for installation.

CHAPTER FOUR
RESEARCH METHODOLOGY

4.1 Introduction

As part of research methodology employed in this study, field measurements were taken to find the sound power level of wind turbine noise emissions and simulations for active noise control. These were carried out and implemented in MATLAB in order to determine the residual noise output(s). The method of active noise control was accomplished by superimposing the anti-noise signal which was generated through the secondary speakers with the noise signal. The system is also made up of other components in order to make the active noise control system to properly function. A microphone that is externally placed somewhere in the wind turbine used to perceive and obtain the noise coming from the blades interaction with the wind. A secondary loudspeaker will then generate another noise signal that interferes destructively with the noise signal.

A noise cancelling secondary speaker was placed at the source of sound to be attenuated. In this case, the audio power levels must be the same as the source of the disturbance. The transducer emitting the cancellation signal may be alternatively be located with the sound source to be attenuated. For a study of this nature, the need to determine the tone levels, masking noise levels, tonality and declaration of sound power levels of the turbine will be required. Also, appropriate experiments will be needed to be carried out to generate specific data which will be validated numerically in order to arrive to a significant conclusion.

4.2 Study Location and Cases

The test wind turbine used for noise analysis for the present study is a three-bladed horizontal axis wind turbine located on the Mariendahl farm about 30km away from Stellenbosch in the Western Cape Province of South Africa. The turbine has a blade diameter of 7.2m and it operates at a fixed speed of 150rpm. The data was acquired using National Instruments Data Acquisition (NI DAQ) and logged using Signal Express. Noise data has been acquired for wind speeds 4.5m/5- 9m/s and background noise for wind speed from 1m/s-4m/s.

The data processing begins with A-weighting the analog signals, which was done to adjust the noise for measurement based on the way humans perceive sound. The data was then time-averaged over 1 second. One third-octave analysis was performed for background and wind noise; next was the computation of the power spectrum followed by the band power. All these are carried out in order to compute the level of noise emitted from wind turbines and if there was a need for control.

To ensure validity of data, the following steps were implemented:

i. Sound level meters and microphones used for the study were covered with primary windscreen in order to reduce contamination of noise from the wind.
ii. Microphones were placed on a plywood board on ground surface in order to reduce reflection from the ground.
iii. Measuring instruments were calibrated in order to give some measure of confidence and authenticity to measured data.
iv. Contaminated data such as sounds from cars, airplanes, human voice and animal sounds were discarded.
v. Wind turbine noise and background noise were logged in similar conditions.
vi. Data was discarded when there was equipment failure.
vii. Data was discarded during periods of rainfall.

4.3 Study Design

The Environmental Noise Protection agency (New York State Department of Environmental Conservation) noise guidance note (NG3) has provided standardized templates for noise analysis while carrying out noise measurements on wind turbine sites in order to be in compliance with the agreed noise limits. Among these noise measurement standards are: *IEC 61400-11, Wind Turbine Generator Systems- Part 11: Acoustic Noise Measurement Techniques*. The methodology for the present study was based on these standards (IEC 61400-11)

4.3.1 Choice of study design

The need for a reliable noise assessment prompted the International Electro-technical Commission (IEC) to establish the first edition of IEC 61400-11 (Lin *et al., 2011).* It has been

said to be the most significant standard relating to wind turbine noise due to the availability of a methodological approach of noise quantification (McAleer *et al.*, 2011). Other methods have proven insufficient and lacking credibility when used for mutual comparison (Lin *et al.,* 2011).

The standard has proven effective in several noise assessments on aerodynamic noise from wind turbines as recorded by researchers (Lee and Lee, 2014). Lin *et al.* (2011) developed an automatic platform for measuring wind turbine noise based on LabVIEW and IEC 61400-11 was the standard used for microphone placements and locations. This was done in order to guarantee uniformity and precision of the measured data.

Another study by Lee and Lee (2014) examined production of aerodynamic noise from small wind turbines. To this effect predictions and measurements were both carried out on a 10kW wind turbine using IEC 61400-11. The measured results gave an applicable measure of noise emitted from the turbine which was in turn compared with predicted data.

4.3.2 Calculation of the masking noise levels $L_{pn,iT}$

The masking noise $L_{pn,I}$ as defined by Swift-Hook (1989) was implemented as:

$$L_{pn} = L_{pn,avg} + 10L_g \left[\frac{critical\ bandwidth}{effective\ noise\ bandwidth}\right] \quad (4.1)$$

where: $L_{pn,avg}$ is the energy average of the spectral lines identified as masking. This was used while carrying out analysis in the next section.

4.3.3 Declaration of sound power level, sound pressure level and tonality levels of wind turbines

The declaration will wind farm planning more reliable and shall also facilitate the relationship of sound power levels and tonality levels of various kinds of turbines.

The sound power level of a source, L_w , according to Swift-Hook (1989) is given by:

$$L_w = 10 \log_{10}\left(\frac{P}{P_0}\right) \quad (4.2)$$

with P equal to the sound power of the source and P_0 a reference sound power (usually 10^{-12} Watts)

The declared sound power levels for a wind turbine was calculated from *n* measurements results $\{L_i\}=1,.....n$ acquired by carrying out one measurement each on *n* similar single turbines. The *n* measurements results in a mean value L_w; a standard deviation *s* was defined as follows:

$$L_w = \sum_{i=1}^{n} \frac{Li}{n} \quad (4.3)$$

$$S = \sqrt{1/(n-1)\sum_{i=1}^{n}(Li - Lw)2} \quad (4.4)$$

The standard deviation of production σ_p was estimated from:

$$\sqrt{(s^2 - \sigma^2)} \leq \sigma_p \leq s \quad (4.5)$$

The standard deviation of reproducibility estimate σ_R, was 0.9dB (IEC 61400-11).

The standard deviation σ used for the declaration was then determined by:

$$\sigma = \sqrt{\frac{1}{n}}({\sigma_R}^2 + {\sigma_P}^2) + ({\sigma_R}^2 + {\sigma_P}^2) \quad (4.6)$$

$$= \sqrt{\frac{1+n}{n}}({\sigma_R}^2 + {\sigma_P}^2) \quad (4.7)$$

with σ_R= 0.9dB and σ_p=s

The declared sound power level was calculated, as given by Swift-Hook (1989):

$$L_{wd} = L_w + k = L_w + 1.645\,\sigma \quad (4.8)$$

The sound pressure level (SPL) of a noise, L_p, is given by Swift-Hook (1989) as:

$$L_p = 20 \log_{10}\left(\frac{p}{p_0}\right) \quad (4.9)$$

with p equal to the effective (or root mean square, RMS) sound pressure and $p0$ a reference RMS sound pressure (usually 20 x 10^{-5}).

When turbulence interacts with either the leading or trailing edge, the type of energy produced is broadband in nature and a turbulence leading-edge interaction noise is produced. The peak energy (Zhu, 2009) for this type of noise was contained at a frequency of:

$$f_{peak} = \frac{StV_{tip}}{h - 0.7R} \quad (4.10)$$

$$\frac{LD_T}{V_{tip\ qcl}} = 2\pi\alpha \frac{D_T}{V_{tip}} \quad (4.11)$$

where:

L Time derivative of lift [-];

D_T Tower diameter [m];

q Dynamic pressure of the flow approaching the blade tip [Pa]; and

c Blade chord [-].

4.4 Procedure for Wind Turbine Noise Measurements

Quantitative data has been collected using noise measuring equipment and this was carried out in accordance with IEC 61400-11. Sound pressure measurements were taken using MA211 preamplifier together with BSWA MP201 microphone. Also a RION sound level meter with a range of measurement from 25-130dBA and a frequency range of 10Hz-20Hz was used for instantaneous sound level measurement. In order to determine the optimal time for noise measurements, the equivalent sound level was recorded for a 7 hour period between 10am-5pm.

4.4.1 Experimental set-up

4.4.1.1 Calibration of microphones and sound level meter

In order to establish the relationship between the signal at the electrical terminal of the microphone and the acoustical signal at its diaphragm or other specified reference positions, microphones and other measuring instruments need to be calibrated. Calibration is important because it gives a level of confidence and authenticity to measured data. And it is an important process while taking measurements using measuring instruments generally (Baath, 2014; Lee and Lee, 2014). The microphones and sound level meter used for this measurements have been calibrated using a Larson Davis 4L200 precision acoustic calibrator. The calibrator has one frequency at 1000Hz and has two dB levels: 94dB and 114dB respectively.

4.4.1.2 Instrumentation location

The wind vane and anemometer are on a tower at a distance 32.9m from the test turbine at a bearing of 290^{o} true. The anemometer was on a height corresponding to the hub height of 18m. The tower is at a distance of 2.5 rotor diameters from the test turbine. This is in the range of 2 and 4 rotor diameters according to IEC 61400 standards. Table 4.1 gives the microphone positions for test turbine and background measurement.

T able 4.1: Microphone positions for turbine and background measurement

Microphone	Distance to Turbine [m]	Slant Distance [m]
Reference	31.6	42.4

4.4.2 Data acquisition

To get the aerodynamic noise, on-site sound pressure measurements were carried out. The system used for noise measurement consists of MA 211 ½" ICP preamplifier. This is a preamplifier with a high impedance input and low inherent noise. It has a frequency with flat response which guarantees high quality measurements that is in accordance with IEC 61672 class 1 requirements. This type of microphone was chosen because it is lower in cost, easy to use and can connect directly to any ICP input channel and transmits signal over a long distance cable length. This is particularly important because measurements were carried out on a farm where the distance in which the microphone was placed to the base of the tower was as long as 31.6m.

Attached to the preamplifier is BSWA MP 201 microphone which can achieve a range of 15dBA to 130dBA; a RION precision handheld sound level meter was also used during the field measurements together with windscreens and an AC power cable of 50m for the power supply. The windscreen consisted of one half of an open cell foam wind screen with a diameter of approximately 90mm, which is centered on the diaphragm of the microphone. National Instrument data acquisition (NI DAQ 9233) module and a computer for data processing and storage were also used for logging the analog input of sound pressure. Figure 4.1 shows the entire field hardware arrangements during the experiment.

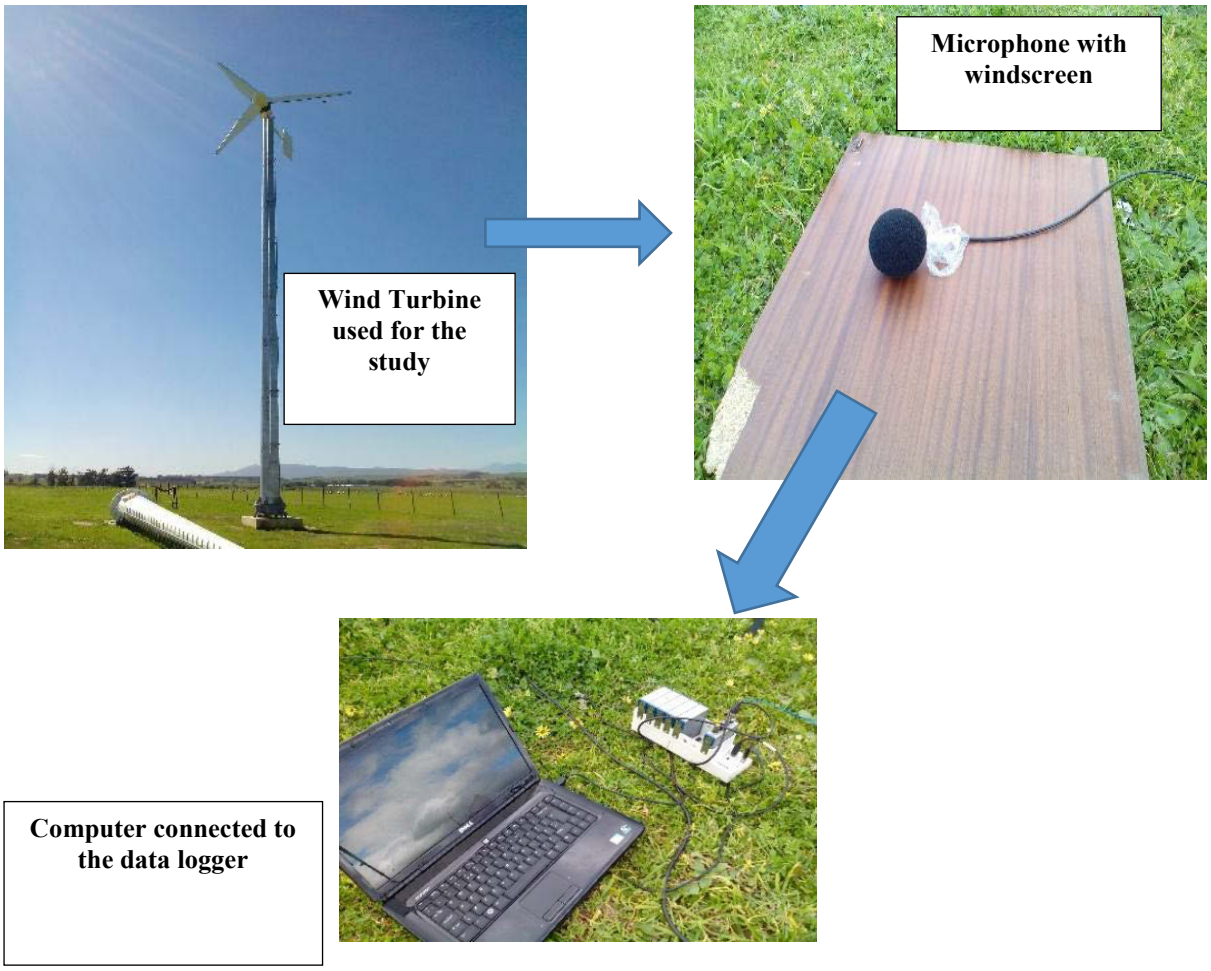

Figure 4.1: Field hardware experimental arrangement and setup

The reference distance R_{ref} is given by Swift-Hook (1989) and IEC 61400-11 as:

$R_{ref} = H + {}^{D}/_{2}$ (For a horizontal axis wind turbine) (4.12)

where H= distance from ground to the centreline of the rotor shaft and

D= diameter of the rotor

The microphones were mounted on a board made of plywood with the diaphragm of the microphone in the vertical plane and with the axis of the microphone pointing towards the wind turbine. The board was placed on the ground with its long sides pointing towards the wind turbine. The positions taken are as shown in Figure 4.2 and Figure 4.3 respectively and were chosen so that the influence of reflecting structures like buildings is minimized (IEC 91400-11).

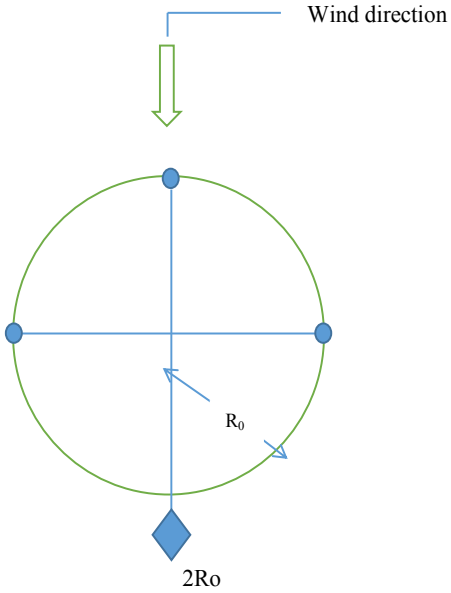

Figure 4.2: Field microphone positions

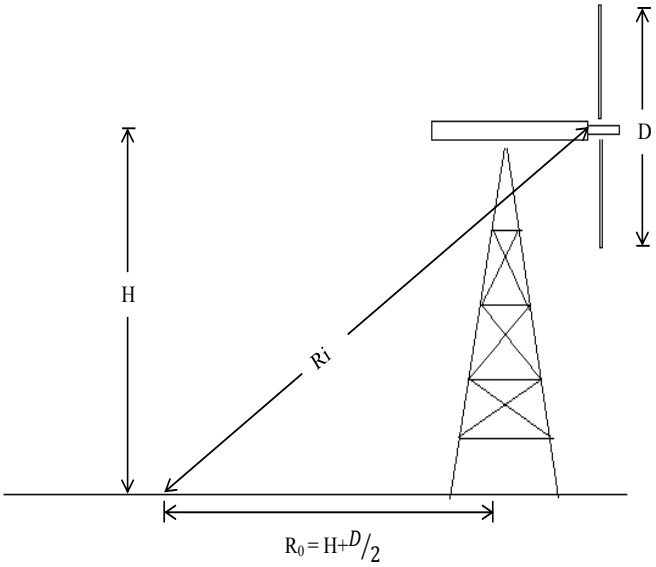

Figure 4.3: Illustrations for the definition of R0 and Ri for a horizontal axis wind turbine (IEC 61400-11)

The entire set-up was connected using the appropriate cables; and measurements were taken at different positions. In order for error to be minimized, a free-field microphone pointed at the source of sound was used. The data was logged using National Instrument Data

Acquisition 9233 which was run using inline LabVIEW software, and data was logged at 1mins interval over a period of time. The noise data was recorded as time signal in time-dependent voltage which was later converted into decibels while carrying out the analysis. This was carried out based on the relationship according to Baath (2013):

$$V_T = P_T g \tag{4.13}$$

where g is the instruments gain factor.

The National Instruments Data Acquisition had four (4) channels or modules and only one of the channels was used for the microphone.

4.5 Data Analysis

In order to get extensive data from the wind turbine, a number of measurements regarding acoustic and meteorological conditions have been undertaken.

While collecting data, background noise was collected at wind speeds below the cut-in speed. Based on the Wind Farms Environmental Noise Guideline (2009), the flow chart in Figure 4.4 was used as a guideline for compliance checking of noise measurement and data reporting. This was done using signal express, analog input analysis.

For Active Noise control, analysis was processed in MATLAB in which simulations were carried out to determine the primary path impulse response, secondary path impulse response, power spectral density plots and residual noise output.

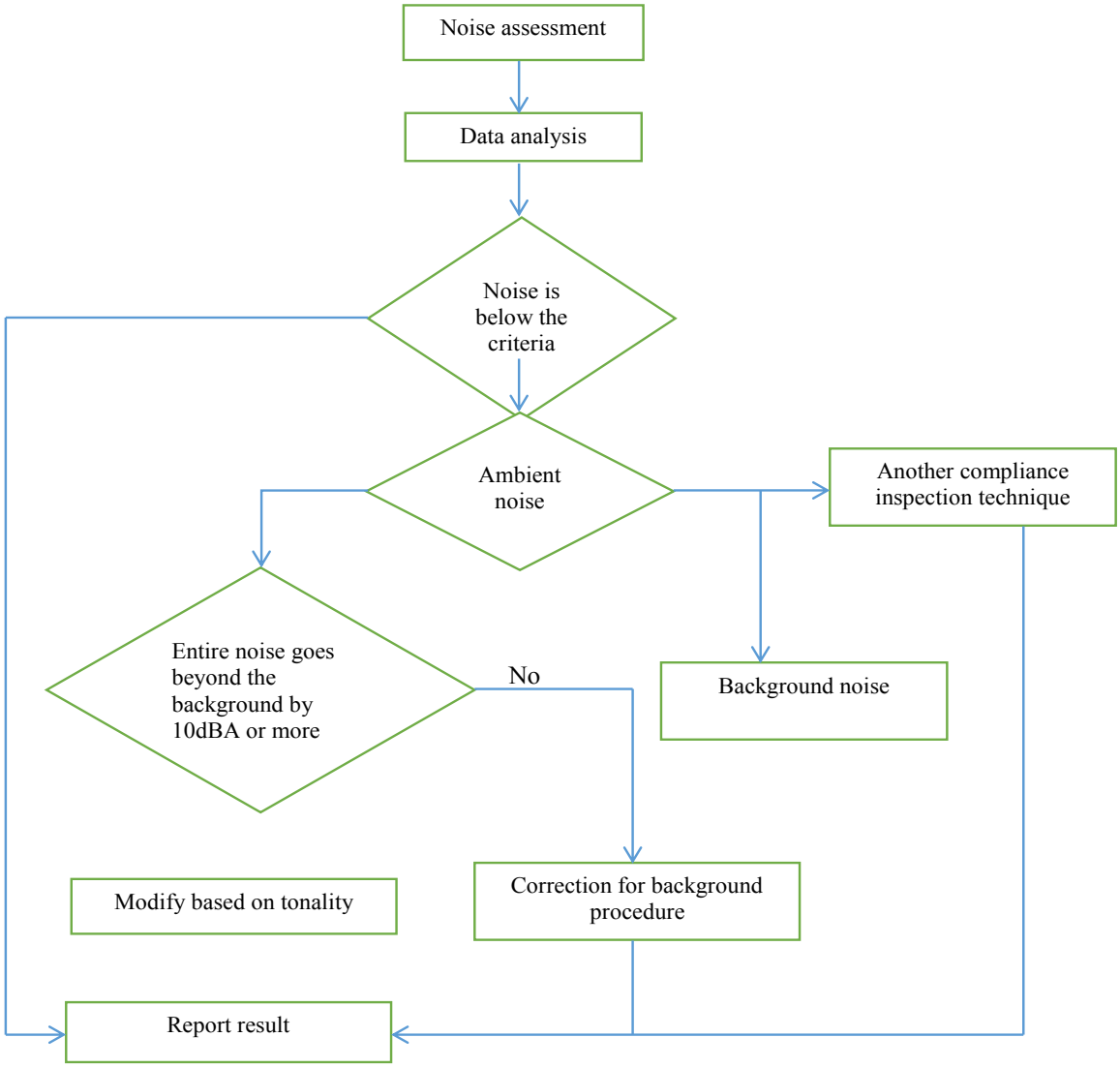

Figure 4.4: Algorithm for compliance checking Source: Wind Farm Environmental Noise Guideline (2009)

4.6 Site Conditions

4.6.1 Wind turbine description

The turbine used for this analysis is of 15kW power, fixed speed turbine running at 15m/s, and having a rotor speed of 150 RPM. Figure 4.5 is a picture of the test turbine in Stellenbosch, case site of the study and Table 4.2 gives the description of the test turbine.

Figure 4.5: Mariendahl Wind Turbine in Stellenbosch

Table 4.2: Wind turbine description

Power	**15kW**
Hub height	28m
Blade diameter (D)	7.2m
Wind turbine rotor placement	Upwind
Wind turbine rotor axis	Horizontal axis
Number of blades	3
Tower type	Tubular

4.6.2 Environmental description

Description of environmental information recorded at the time of study and roughness length of ground are presented in Table 4.3.

Table 4.3: Environmental descriptions

Air pressure [hPa]	1020
Relative air humidity [%]	49
Temperature [^{o}C]	20
Roughness length, z_o [m]	0.05

4.6.3 Instrumentation

The instrumentation used for the experimental testing are listed in Table 4.4.

Table 4.4: List of instruments and equipment used for field study

Instrument name	**Serial Number**
Larson Davis 4L200 calibrator	4233
MA 211 1/2" ICP Preamplifier	24519
BSWA MP 201 microphone	450466
RION Precision Sound Level Meter	11030741
NI DAQ 9233 Data acquisition	135c146

4.7 Summary

This Chapter describes the study design that has been used for the field study, and also justification for their application. It goes on to explain the determination of the masking noise levels, determination of the tonality and declaration of the sound power level. The procedure used for the noise measurements based on IEC 61400-11 was presented, together with the

experimental set-up, calibration of the instruments and the positioning of the reference microphone. Section 4.3.2 is the procedure used to acquire data from NI-DAQ 9233 and how data was analyzed is given in section 4.4. Section 4.5 presents the conditions of the measurement site. These included the test wind turbine description, environmental description and equipment description. Chapter 5 will consist of results of simulation for active noise control, in which one reference microphone was used. Also results obtained via inline LabVIEW are also presented for sound level measurements from noise measurements which were carried out on the test turbine.

CHAPTER FIVE
RESULTS AND DISCUSSIONS

5.1 Introduction

This chapter begins with the results obtained while taking noise measurements from the test turbine in Stellenbosch, Cape Town. The analyses of these measurements are also carried out, which consists of the wind speed, one-third octave analysis and sound pressure analysis. From the analysis it can be seen that the major components of the noise is in the low-frequency range. Having established this, section 5.5 presents a simulation model of an active noise control system which has been validated against experiment. The simulation results presented is not capable of reproducing phenomena taking place inside the control system because it was simulated in MATLAB. For instance, the limitations of the computational capabilities of a digital signal processor were not taken into account.

5.2 Wind Speed

The analysis of wind speed around a wind turbine is important because radiated noise is in relation to the wind speed experienced by the turbine (ETSU). Wind speed was measured from an anemometer which was placed on a mast, 10m high (IEC 61400-11). The height of the mast was chosen to be 10m. This was to ensure that there were no interferences between the rotor wakes and upwind of other turbines (ETSU). This distance also produces uniformity during the measurement and evaluation. Figure 5.1 presents the wind speed measured on the test site while carrying out noise measurement. From the test results as indicated in Figure 5.1, the highest wind speeds were between 10:00hrs and 15:00hrs and noise measurements were taken during this period of time.

5.3 One-third Octave Analysis.

The one-third octave band spectrum was used to examine the strength at various frequencies for both the wind turbine noise while in operation and the background noise. It consists of the entire audible frequency range. One-third octave analysis is accepted because of its repeatability and suitability used for visual inspection and comparison. From Figure 5.2 the

one-third octave band spectrum for wind turbine noise is shown with the highest frequency component at 257Hz which is in the low frequency range and at a band power of 46dBA.

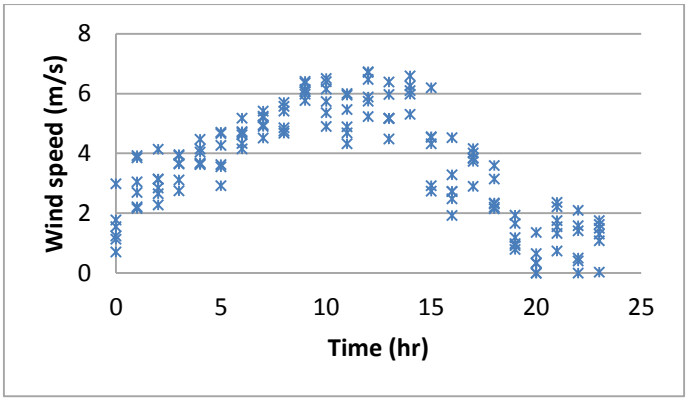

Figure 5.1: Wind speed

While Figure 5.3 presents the one-third octave band spectrum for background noise (when turbine was parked) gives the highest frequency at 500Hz corresponding to a sound pressure level of 22.5dBA.

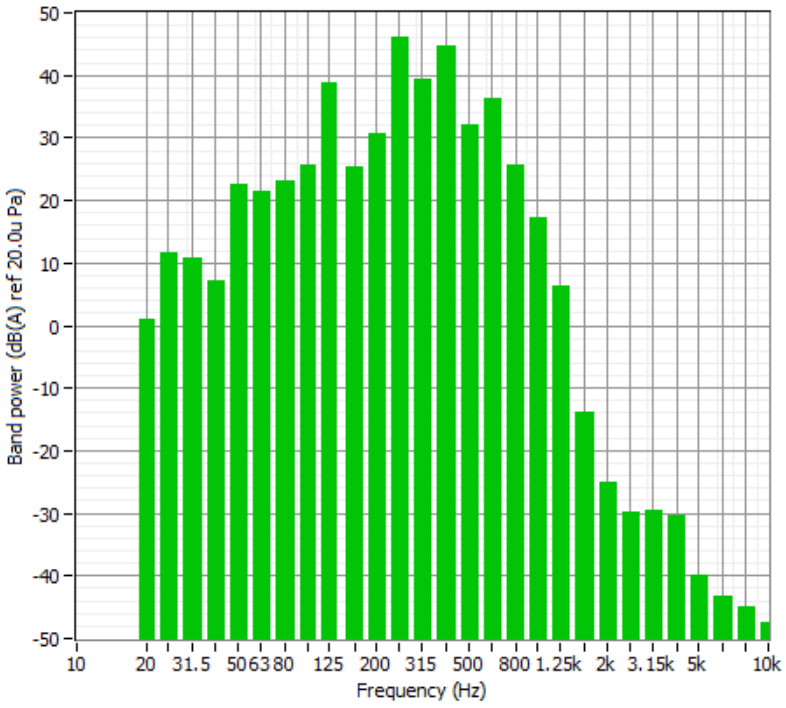

Figure 5.2: One-third octave band spectrum for wind turbine noise

The one-third octave analysis performed supports the argument that low frequency noise from wind turbines should be addressed because they travel farther and have been said to

cause annoyance and psychological effects in humans residing in close proximity to where they are installed.

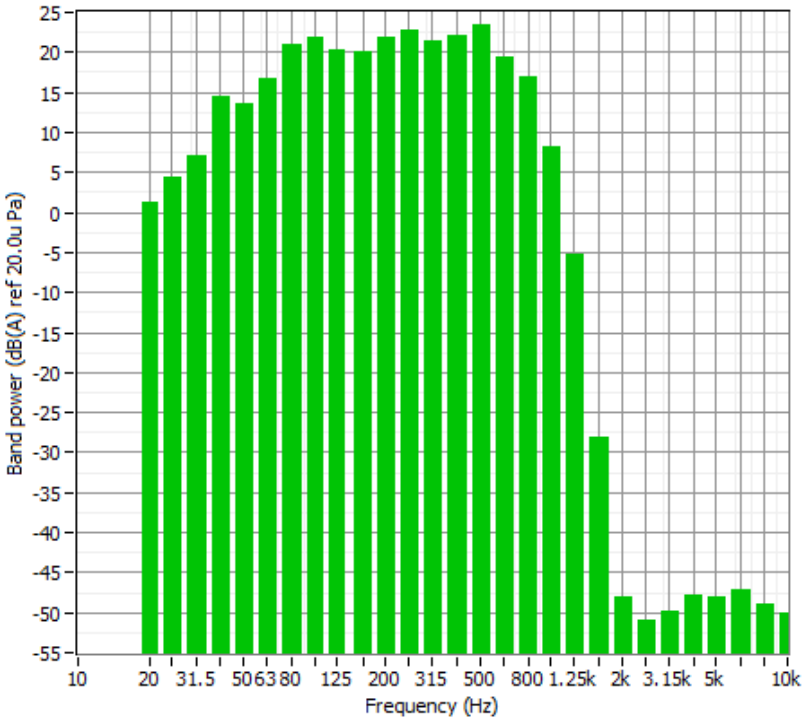

Figure 5.3: One-third octave analysis for background noise

5.4 Sound Pressure Analysis

This section presents analysis on sound pressure measurements. The equivalent noise level as measured at some distances away from the foot of the tower is shown in figure 5.4. The mean level downstream is 58dB (+1 or-1) for distances 0, 10, 15 and 30m away from the foot of the turbine. This figure shows that sound is attenuated further away from the source, having the highest value at the foot of the tower.

The reason for increased level of noise at the foot of the tower has been attributed to mechanical noise and vibration from the tower casing. Another cause of increased noise is also due to the interaction between the blades as it passes the tower which produces a thumping sound. Figure 5.4 is the sound pressure measured at 1s interval for over 4 minutes and averaged over a period of 1sec. The data hasn't been filtered and the variation in equivalent sound level with time is typical for what was measured around the turbine then averaged over the time presented. The value of the sound pressure level was computed using the equation 4.8 from section 4.2.4.

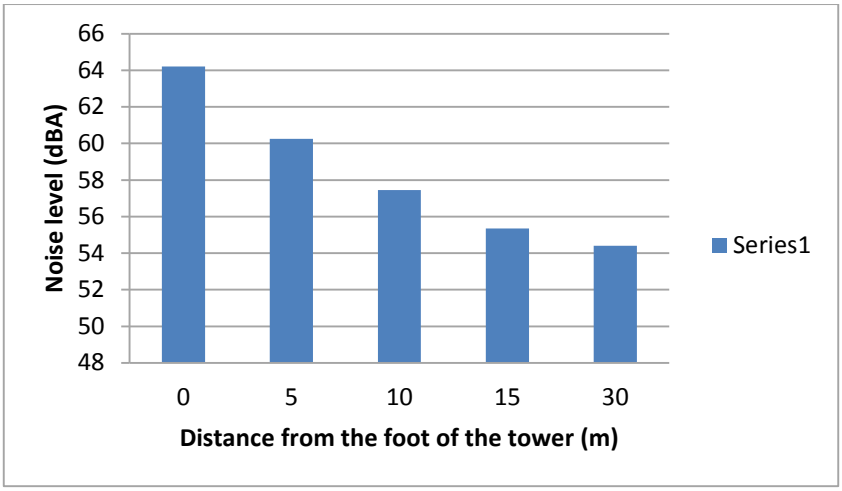

Figure 5.4: A-weighted sound level measured at some distances away from foot of the tower

From Figure 5.5, the highest value of sound pressure level is 480mPa and is equivalent to 67.6dB. This value exceeds the proposed cumulative site and turbine noise limits as compiled in the document by the Environmental Protection (EPA NG3), which states that daytime noise level should not exceed 55dB.

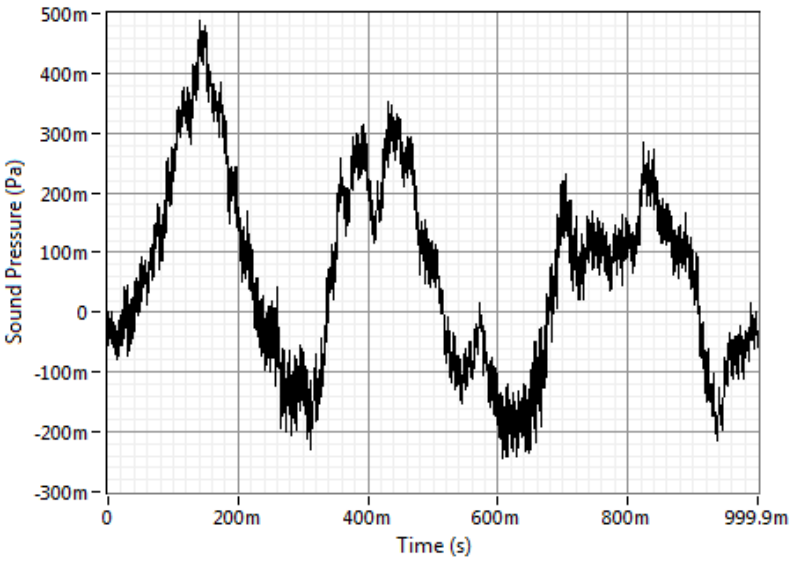

Figure 5.5: Spectrum of sound pressure of wind turbine noise

The strength of the energy variation as a function of frequency is given in Figure 5.6. From the figure, the energy is strongest in the first 0-500Hz and weakest at 12kHz.

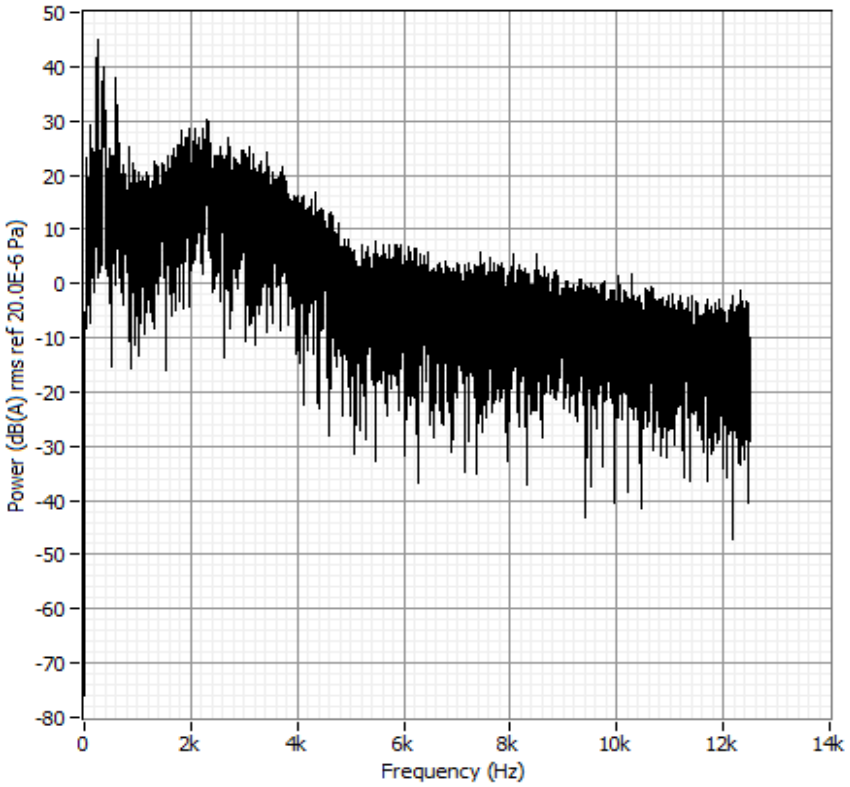

Figure 5.6: Power spectrum of wind turbine noise

5.5 Active Noise Control Simulations

The performance of a Filtered-x Least Mean Squared (FXLMS) algorithm in reducing wind turbine aerodynamic noise is illustrated in this section. The results presented are based on the inversion of the linearized model discussed in section 2. ANC scenarios are simulated in a MATLAB environment. The impulse responses of the primary, secondary and secondary path estimates were simulated (Fig. 5.7, 5.8, 5.9 and 5.10).

For this simulation, the noise was sampled at 22050Hz for 2 sec and it combines the noise signal, the FXLMS filter and the primary path filter. An FIR filter was used for the primary propagation path, and it was band limited from 200 to 800Hz and for the secondary path, it was 160 to 2000Hz. The simulation was in three stages: importation of the noise signal into MATLAB workspace, processing the noise through the primary filter and finally processing the output through FXLMS filter.

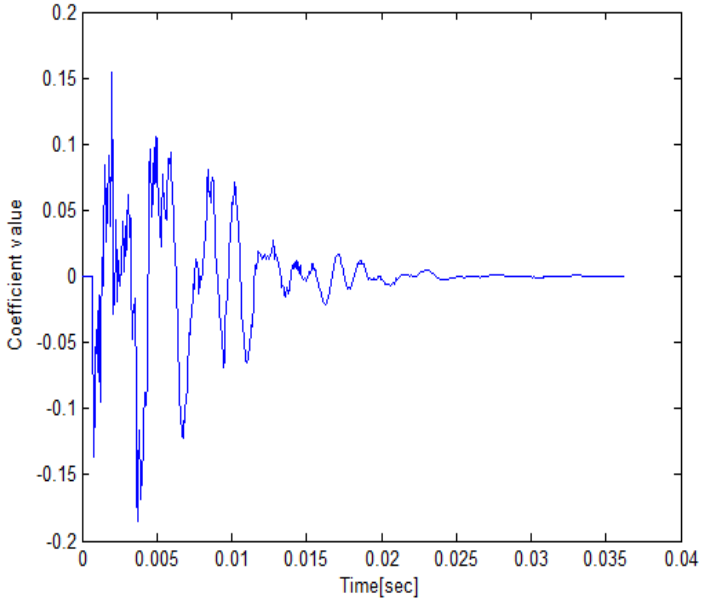

Figure 5.7: Primary path impulse response

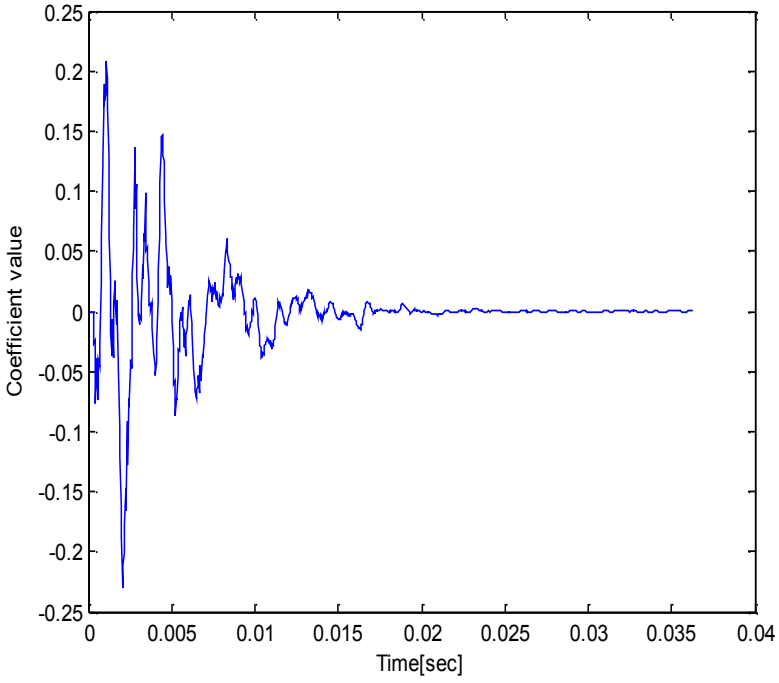

Figure 5.8: True secondary path impulse response

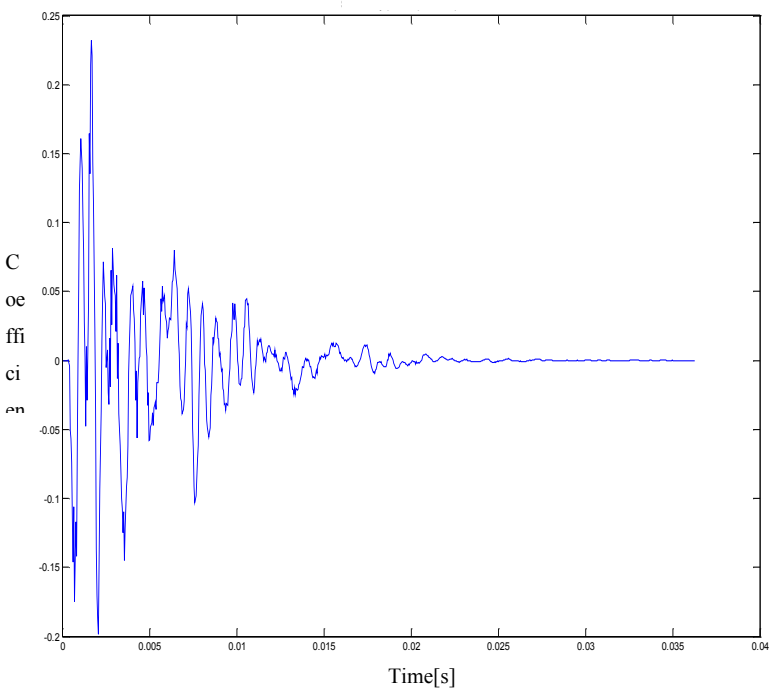

Figure 5.9: Secondary path impulse response

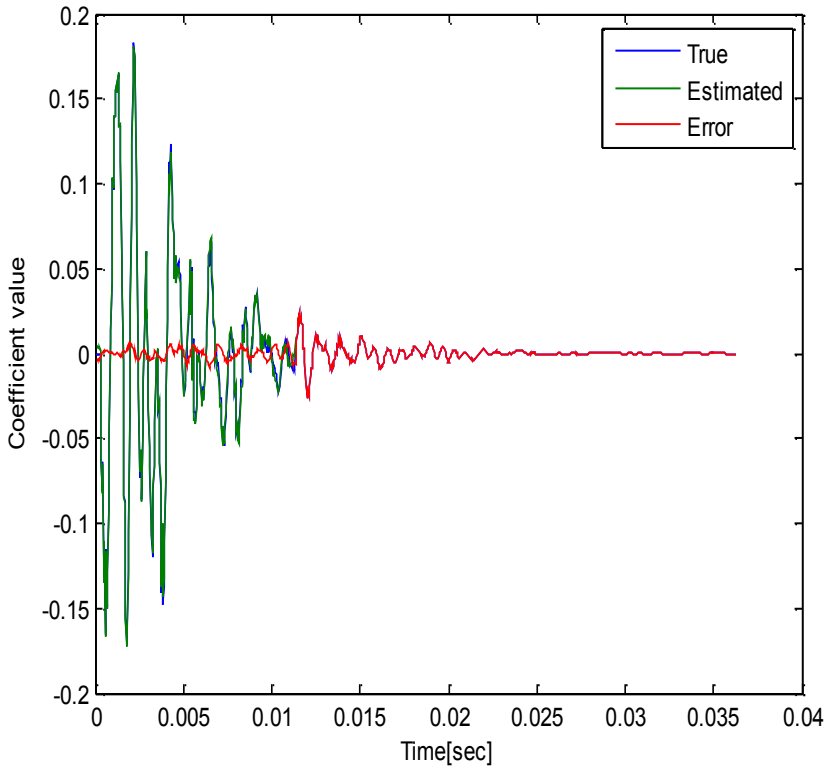

Figure 5.10: Secondary path impulse response estimation

Even though a wide range of algorithms can be used to design the secondary propagation path estimate, the Normalized LMS algorithm was used because of its robustness and simplicity. Plots of output and error signals are shown in Figure 5.11.

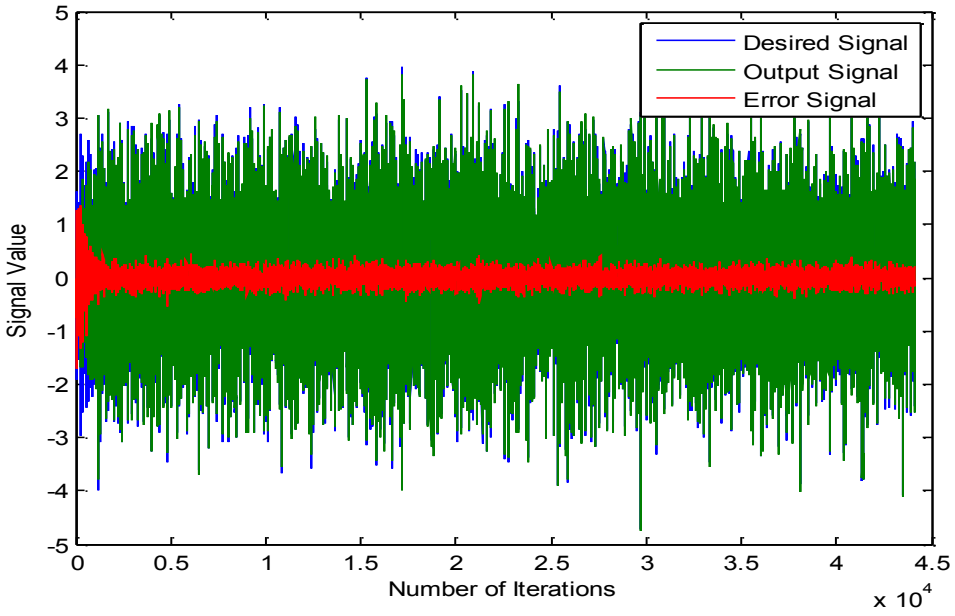

Figure 5.11: Secondary identification using NLMS algorithm

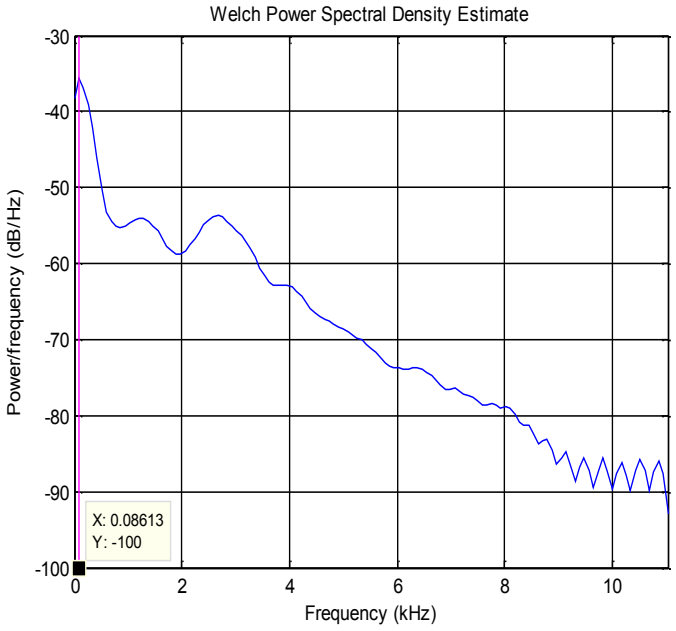

Figure 5.12: Power spectral density

The Welch Power Spectral Density (PSD) estimation using spectral estimates of the signal was computed. Then the highest frequency was found by looking at the spectral density and

locating the frequency at which the PSD reaches its highest value, this was found to be at 0.08613 KHz (86.13Hz). This is therefore the "true frequency". This continuous wavelet transform of the signal was computed and the spectral information is presented in Figure 5.12, while Figure 13 shows the spectrum of the original and attenuated noise signal.

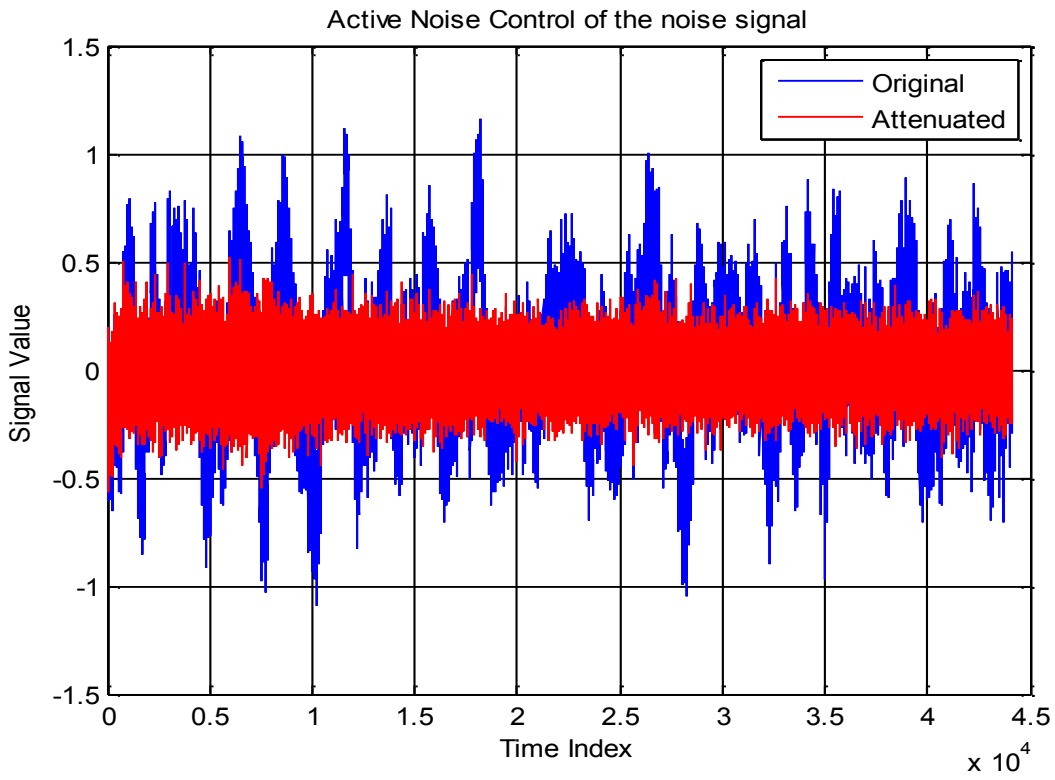

Figure 5.13: Original and attenuated noise

For the MATLAB implementation the frequency domain plots above represents information about the turbine aerodynamic noise magnitude and phase at each frequency. The magnitude response shows the strength of the frequency components while the phase shows how all the frequency components aligns in time. From Figure 5.14(a), it can be seen that the highest magnitude of noise is found between 0 to 200 Hz. This indicates that the noise has low frequency components. Figure 5.14 and Figure 5.15 shows the magnitude and phase responses for both the original and attenuated signals.

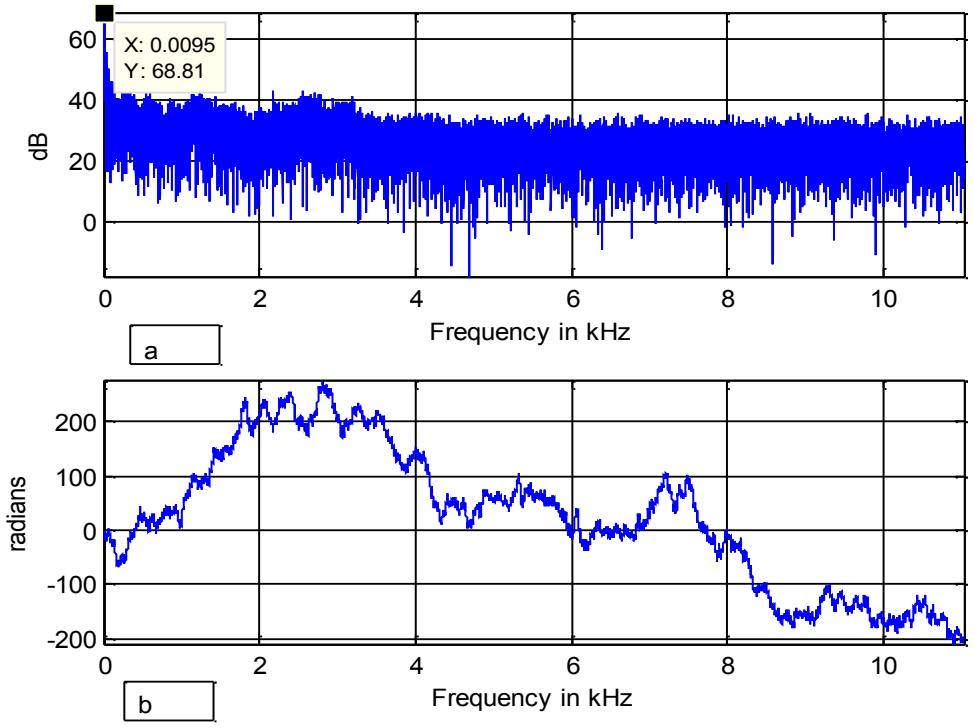

Figure 5.14: Magnitude (a) and phase (b) response of the original signal

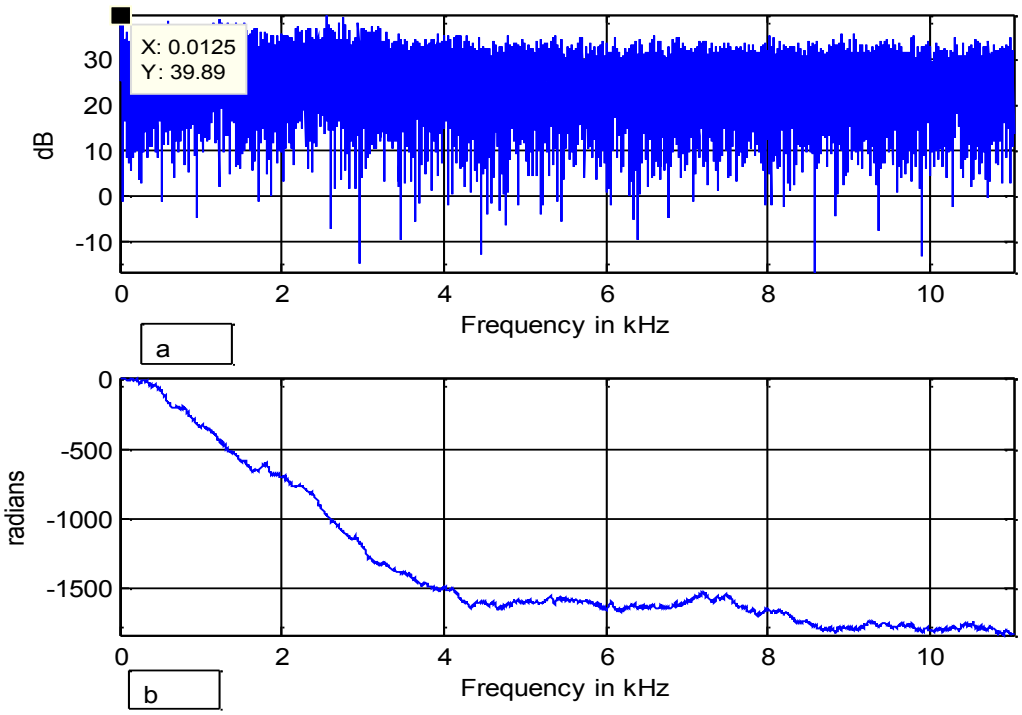

Figure 5.15: Magnitude (a) and phase (b) of the attenuated signal

5.6 Summary

In this Chapter, the findings related to each research objective were analyzed. The time of the day with the highest wind speeds were between 10:00hrs and 15:00hrs, and sound pressure measurements were carried out during this period. Comparison of one-third octave spectrum of the wind turbine noise shows a higher strength of sound power at 257Hz and 500Hz for wind turbine and background noise respectively. From the analysis of sound pressure, it has been shown that sound emanating from a point source is attenuated with an increase in distance. From figure 5.4, the highest sound pressure is 67.6dB which exceeds the noise limit given in EPA NG3 document. The active noise control simulation was implemented using FXLMS algorithm. NLMS algorithm was used to update the adaptive filter coefficient. Results show a minimization in residual error with a noise reduction of about 29dB.

CHAPTER SIX
CONCLUSIONS AND RECOMMENDATIONS

As the development in wind energy increases globally, solutions and more understanding are sought continuously on the complexities and general effects of wind turbine noise. To understand this problem, studies and evaluations of the source of this type of noise is required. Wind turbine noise consists of low frequency and high frequency noise and this study focuses on reducing the noise in the low frequency range. It is believed that this study provides some further understanding to this effect.

This research has implication for health issues as the low frequency noise is said to cause fatigue and restlessness in humans and also low work performance. A basic knowledge of the characteristics of wind turbine noise, under several conditions, presents an immense opportunity for wind turbine operators and manufacturers as well.

The study of wind turbine noise is an opportunity to build knowledge and keep driving renewable energy. The conclusions, recommendations and future work that follow in the proceeding sections serve to enhance current knowledge and present some opportunities for the future.

6.1 Conclusions

The research statement, as formulated in section 1.7 is “Active Noise Control (ANC) can be used on wind turbines to reduce low frequency noise” and the research objectives listed in section 6.1 were achieved.

This study has been conducted to investigate the potentiality of using ANC on wind turbines for low frequency noise reduction. To this end, a wind turbine noise assessment was carried out on a test turbine facility in Stellenbosch, Capetown, South Africa and the procedure was based on IEC 61400-11 standard.

The results in the present study have been found to be in line with much of results from previous studies on wind turbine noise discussed in chapter two. Passive methods that have been used are also studied. Conclusions have been made on the fact that these passive methods work well in reducing high frequency noise but are inefficient in reducing the low

frequency noise from wind turbines. Active noise control however works well in reducing low frequency noise. Past studies that have implemented ANC are studied and the importance of a proper control system has also been explained.

The analysis of wind turbine noise is presented and a root cause approach has been implemented. The sources of mechanical and aerodynamic noise have been studied and it has been shown that mechanical noise is no longer an issue for modern wind turbines as they are being designed to minimize mechanical noise. However, aerodynamic noise is still an issue that is still receiving an active research. Some of these aerodynamic noises are low frequency, which have been shown from Figure 5.2 to be within the range of 20-500Hz in nature and are the main sources of vibration. This has led to a need for more critical analysis of low frequency aerodynamic noise. Analyses were conducted to look at four key areas: sound propagation distance, sound pressure level, one-third octave band spectrum and simulations in active noise control using MATLAB. The data allowed for observations to be made on the wind turbine noise. It was shown that the low frequency noise had the highest band power of 46dBA and is the major cause of disturbance, annoyance and loss of concentration. This justifies the fact that low frequency noise should be seriously taken into consideration in further analysis.

The procedure used for the noise measurements based on IEC 61400-11 is stated, emphasizing the experimental set-up, the noise measuring instruments were calibrated using the Larson Davis 4L200 calibrator to ensure the measurements had a high degree of confidence. The reference microphone was located 31.6m away from the foot of the turbine.

The time of the day with the highest wind speeds while noise study from the test turbine was carried out is shown to be between 10:00hrs and 15:00hrs. Comparison of one-third octave spectrum of the wind turbine noise shows a higher strength of sound power at 257Hz and 500Hz for wind turbine and background noise respectively. From the analysis of sound pressure, it has been shown that sound emanating from a point source is attenuated with an increase in distance. The highest sound pressure is 67.6dB which exceeds the noise limit given in EPA NG3 document.

An active noise control system is proposed for reducing the noise level from wind turbine blades using the FXLMS adaptive filter. The input to the system is noise signal which was measured according to IEC 61400-II standard and NLMS algorithm was used for updating filter coefficients. The implementation in MATLAB environment has been described.

FXLMS algorithm was able to minimize residual error. The results of the simulation show that noise was reduced by about 29dB. The Welch power spectral density estimate using spectral estimation of the signal was computed and the main frequency was found to be 86.13Hz also referred to as the true frequency. From the MATLAB simulations the highest magnitude of noise was found to be between 0-200Hz.

6.2 Recommendations

The behavior of the ANC at a very high sampling frequency should be further investigated along with a more parametric study. The use of a variable speed turbine should be considered in subsequent studies as a fixed speed turbine running at 150rpm was used for the current study. As a result, proper sound power and regression analysis could not be carried out.

The use of other algorithms with good stability criteria and also different step sizes should be considered.

Multiple reference active noise control is mainly used in complex systems, in which there are multiple reference noise sources. The sources of noise from wind turbines will have a significant impact on the quality of the reference signals. Future work should consider the use of multiple sensors in acquiring noise signals from different locations from wind turbine blades. Also it is recommended that optimization of reference sensor location be studied. The basic optimization criterion would be achieving maximum reduction of noise with minimum reference sensors while keeping the reference signals as uncorrelated as possible.

The study of efficient algorithms is essential when dealing with a complex system such as a wind turbine. An example of algorithm that could be used is the domain block algorithm which is efficient for multiple reference active noise control.

REFERENCES

Abdullah, A., & Fekih, A. (2013). *An overview of the current state of wind energy technology development in the US.* Paper presented at the Green Technologies Conference, 4-5 April, 2013, Denver Colorado.

Akhtar, M. T., Abe, M., & Kawamata, M. (2005). A method for online secondary path modeling in active noise control systems *in: Proceedings of the IEEE International Symposium on Circuits and Systems, ISCAS* 23-26 May 2005, Kobe, Japan.

Apolinário Jr, J. A. (2009). *QRD-RLS Adaptive Fltering* (Vol. 1978): Springer.

Arakawa, C., Fleig, O., Iida, M., & Shimooka, M. (2005). Numerical approach for noise reduction of wind turbine blade tip with earth simulator. *Journal of the Earth Simulator, 2*(3), 11-33.

Arezes, P. M., Bernardo, C., Ribeiro, E., & Dias, H. (2014). Implications of wind power generation: Exposure to wind turbine noise. *Procedia-Social and Behavioral Sciences, 109*, 390-395.

Pathak, M.B. & Hirave, P. P. (2012). FXLMS algorithm for feed-forward active noise cancellation. *Proceedings of the International Conference on Advances in Computer, Electronics and Electrical Engineering,* 7-9 July 2012, Uttarakhand, India.

Baath, L. (2013). Noise spectra from wind turbines. *Renewable Energy, 57*, 512-519.

Behera, S. B., Das, D. P., & Rout, N. K. (2014). Nonlinear feedback active noise control for broadband chaotic noise. *Applied Soft Computing, 15*, 80-87.

Bengtsson, J. (2004). Is a "pleasant" low-frequency noise also less annoying? *Journal of Sound and Vibration, 277*(3), 535-537.

Bengtsson, J., Persson Waye, K., & Kjellberg, A. (2004). Evaluations of effects due to low-frequency noise in a low demanding work situation. *Journal of Sound and Vibration, 278*(1), 83-99.

Berglund, B., Hassmen, P., & Job, R. S. (1996). Sources and effects of low-frequency noise. *The Journal of the Acoustical Society of America, 99*(5), 2985-3002.

Bo, L., Liu, X., & He, X. (2011). Measurement system for wind turbines noises assessment based on LabVIEW. *Measurement, 44*(2), 445-453.

Brooks, T. F., & Burley, C. L. (2001). Rotor broadband noise prediction with comparison to model data. *AIAA Paper, 2210*, 28-30.

Brooks, T. F., & Hodgson, T. (1981). Trailing edge noise prediction from measured surface pressures. *Journal of Sound and Vibration, 78*(1), 69-117.

Brooks, T. F., Pope, D. S., & Marcolini, M. A. (1989). *Airfoil self-noise and prediction* (Vol. 1218): National Aeronautics and Space Administration, Office of Management, Scientific and Technical Information Division.

Chang, C.-Y., & Luoh, F.-B. (2007). Enhancement of active noise control using neural-based filtered-X algorithm. *Journal of Sound and Vibration, 305*(1), 348-356.

Cheong, C., & Joseph, P. (2014). Cyclostationary spectral analysis for the measurement and prediction of wind turbine swishing noise. *Journal of Sound and Vibration, 333*(14), 3153-3176.

IEC 61400-11 (2006) *Wind Turbine Generator Systems-Part 11: Acoustic Noise Measurement Techniques*. 2nd ed (International Technical Commission, Geneva, 2002 Plus Amendment 1 2006).

Di, G.Q., Li, Z.G., Zhang, B.J., & Shi, Y. (2011). Adjustment on subjective annoyance of low frequency noise by adding additional sound. *Journal of Sound and Vibration, 330*(23), 5707-5715.

Doolan, C. J., Moreau, D. J., & Brooks, L. A. (2012). Wind turbine noise mechanisms and some concepts for its control. *Acoustics Australia, 40*(1), 7-13.

Douglas, S. C. (1999). Introduction to adaptive filters. *Digital Signal Processing Handbook, CRC Press*.

Eleni, D. C., Athanasios, T. I., & Dionissios, M. P. (2012). Evaluation of the turbulence models for the simulation of the flow over a National Advisory Committee for Aeronautics (NACA) 0012 airfoil. *Journal of Mechanical Engineering Research, 4*(3), 100-111.

Errasquin, L. A. (2009). *Airfoil self-noise prediction using neural networks for wind turbines* (Doctoral dissertation, Virginia Polytechnic Institute and State University).

Erkan, F. (2009). *Design and implementation of a fixed point digital active controller headphone.* (Masters thesis), Middle East Technical University.

Friman, M. (2011). *Directivity of sound from wind turbines.* (Masters thesis), Marcus Wellenber Laboratory for Sound and Vibration Research.

George, N. V., & Panda, G. (2013). Advances in active noise control: A survey, with emphasis on recent nonlinear techniques. *Signal Processing, 93*(2), 363-377.

Gérard, A., Berry, A., & Masson, P. (2005a). Control of tonal noise from subsonic axial fan. Part 1: Reconstruction of aeroacoustic sources from far-field sound pressure. *Journal of Sound and Vibration, 288*(4), 1049-1075.

Gérard, A., Berry, A., & Masson, P. (2005b). Control of tonal noise from subsonic axial fan. Part 2: Active control simulations and experiments in free field. *Journal of Sound and Vibration, 288*(4), 1077-1104.

Geyer, T., Sarradj, E., & Fritzsche, C. (2010). Measurement of the noise generation at the trailing edge of porous airfoils. *Experiments in Fluids, 48*(2), 291-308.

Göçmen, T., & Özerdem, B. (2012). Airfoil optimization for noise emission problem and aerodynamic performance criterion on small scale wind turbines. *Energy, 46*(1), 62-71.

Hanning, C. D., & Evans, A. (2010). Wind turbine noise. *Policy, 38*, 2520-2527.

Hansen, C., & Snyder, S. (1997). Active control of noise and vibration, *E&FN Spon, London*.

Hashemian, R. (1996). Design of an active noise control system using combinations of DSP and FPGAs. *In PLD Conference Proceedings,* Nothern Illinois University, Actel Corporation.

Heier, S. (1998). Grid integration of wind energy conversion systems. Publisher: John Wiley and Sons, *ISBN 0, 471 97143*.

Howe, M. (1991). Aerodynamic noise of a serrated trailing edge. *Journal of Fluids and Structures, 5*(1), 33-45.

Huff, D. L. (2007). Noise reduction technologies for turbofan engines. *NASA Technical Memorandum 214495, 1-10.*

Jacobsen, F., Poulsen, T., Rindel, J. H., Gade, A. C., & Ohlrich, M. (2007). Fundamentals of acoustics and noise control. *Ørsted: DTU, Technical University of Denmark*.

Jakobsen, J. (2005). Infrasound emission from wind turbines. *Journal of Low Frequency Noise, Vibration and Active Control, 24*(3), 145-155.

Jianu, O., Rosen, M. A., & Naterer, G. (2012). Noise pollution prevention in wind turbines: status and recent advances. *Sustainability, 4*(6), 1104-1117.

Johansson, S. (1998). *Active noise control in aircraft: Algorithms and applications.* Licentiate Thesis, Blekinge Institute of Technology.

Klug, H. (2002). *Noise from wind turbines standards and noise reduction procedures.* Paper presented at the Forum Acusticum, Sevilla, Spain.

Kong, X., & Kuo, S. M. (1999). Study of causality constraint on feedforward active noise control systems. *Circuits and Systems II: Analog and Digital Signal Processing, IEEE Transactions on, 46*(2), 183-186.

Krstajic, B., Zecevic, Z., & Uskokovic, Z. (2013). Increasing convergence speed of FxLMS algorithm in white noise environment. *AEU-International Journal of Electronics and Communications, 67*(10), 848-853.

Kuo, S. M. (1999). Active noise control system and method for on-line feedback path modeling and on-line secondary path modeling: Google Patents.

Kuo, S. M., Panahi, I., Chung, K. M., Horner, T., Nadeski, M., & Chyan, J. (1996). Design of active noise control systems with the TMS320 family. *Texas Instruments*.

Laratro, A., Arjomandi, M., Kelso, R., & Cazzolato, B. (2014). A discussion of wind turbine interaction and stall contributions to wind farm noise. *Journal of Wind Engineering and Industrial Aerodynamics, 127*, 1-10.

Lauchle, G. C., MacGillivray, J. R., & Swanson, D. C. (1997). Active control of axial-flow fan noise. *The Journal of the Acoustical Society of America, 101*(1), 341-349.

Lee, S., & Lee, S. (2014). Numerical and experimental study of aerodynamic noise by a small wind turbine. *Renewable energy, 65*, 108-112.

Lee, S., Lee, S., & Lee, S. ((2013)). Numerical modelling of wind turbine aerodynamic noise in the time domain. *Journal of Acoustical Society of America, 133*(2), 6.

Leloudas, G., Zhu, W. J., Sørensen, J. N., Shen, W. Z., & Hjort, S. (2007). Prediction and reduction of noise from a 2.3 MW wind turbine. *In Journal of Physics*: Conference Series (Vol. 75, No1,p.012083). IOP Publishing.

Leventhall, G., Pelmear, P., & Benton, S. (2003). A review of published research on low frequency noise and its effects. Department for environment, Food and Rural affairs, London, UK.

Li, X., Qiu, X., Leclercq, D., Zander, A. C., & Hansen, C. H. (2006). Implementation of active noise control in a multi-modal spray dryer exhaust stack. *Applied Acoustics, 67*(1), 28-48.

Lloyd, T., Gruber, M., Turnock, S., & Humphrey, V. (2012). Simulation of inflow turbulence noise. University of Southampton

Lopez-Gaudana, E., Betancourt, P., Cruz, E., Nakano-Miyatake, M., & Perez-Meana, H. (2008). *An active noise cancelling algorithm with secondary path modeling*. 12th WSEAS Int. Conf. on Computers, July 23-25, Grecia.

Manwell, J., McGowan, J., & Rogers, A. (2002). Aerodynamics of wind turbines. *Wind Energy Explained: Theory, Design and Application*, 83-140.

McAleer. S., T. F., McKenzie, A., & McKenzie, H. (2011). *Guidance note on noise assessment of wind turbine operations at EPA Licensed sites (NG3)*.

Meir, R., Legerton, M., Anderson, M., Berry, B., Bullmore, A., Hayes, M., . . . Spode, D. (1996). The assessment and rating of noise from wind farms. *The Working Group on Noise from Wind Turbines, UK, Final Rep. UK-ETSU-97*.

Møller, H., & Pedersen, C. S. (2011). Low-frequency noise from large wind turbines. *The Journal of the Acoustical Society of America, 129*(6), 3727-3744.

Moriarty, P., & Migliore, P. G. (2003). *Semi-empirical aeroacoustic noise prediction code for wind turbines*: National Renewable Energy Laboratory Golden, CO, USA.

Murthy, M. S., Elnourani, M.G.A. (2008). *Active Noise Control of a Radial Fan.* (Masters Thesis), Blekinge Institute of Technology.

Narula, V., Sagar, M., Joshi, P., Mehta, P. S., & Tripathi, S. (2012). Real-time active noise cancellation with simulink and data acquisition toolbox. *ACEEE International Journal on Control System and Instrumentation, 3*(2).

Norton, M. P., & Karczub, D. G. (2003). *Fundamentals of noise and vibration analysis for engineers*: Cambridge university press.
Oerlemans, S. (2011). *Wind turbine noise: primary noise sources.* National Aerospace Laboratory, Armsterdam.
Oerlemans, S., Fisher, M., Maeder, T., & Kögler, K. (2009). Reduction of wind turbine noise using optimized airfoils and trailing-edge serrations. *AIAA journal, 47*(6), 1470-1481.
Oerlemans, S., & Migliore, P. (2004). Wind tunnel aeroacoustic tests of six airfoils for use on small wind turbines. *Report of the National Renewable Energy Laboratory NREL/SR-500-35339*.
Pawlaczyk-Łuszczyńska, M., Dudarewicz, A., Waszkowska, M., Szymczak, W., & Śliwińska-Kowalska, M. (2005). The impact of low frequency noise on human mental performance. *Inter J Occup Med Environ Health, 18*(2), 185-198.
Pearson, C. (2014). *Vertical axis wind turbine acoustics* (Doctoral Dissertation, Cambridge University).
Persson Waye, K., & Rylander, R. (2001). The prevalence of annoyance and effects after long-term exposure to low-frequency noise. *Journal of Sound and Vibration, 240*(3), 483-497.
Ragheb, M. (2011). Vertical axis wind turbines. *University of Illinois at Urbana-Champaign, 1*.
Rogers, A. L., & Manwell, J. F. . (2004). Wind turbine noise issues (Publication). from Renewable Energy Research Laboratory http://www. ceere. org/rerl/publications/whitepapers/WindTurbineNoiseIssues. pdf.
Rogers, T., & Omer, S. (2012). The effect of turbulence on noise emissions from a micro-scale horizontal axis wind turbine. *Renewable Energy, 41*, 180-184.
S. Kottayi, N. K. N. (2012). ANC system for noisy speech. *Signal and Image Processing: An International Journal (SIPJ), 3*, 9.
Salt, A. N., & Hullar, T. E. (2010). Responses of the ear to low frequency sounds, infrasound and wind turbines. *Hearing Research, 268*(1), 12-21.
Schepers, J., Curvers, A., Oerlemans, S., Braun, K., Lutz, T., Herrig, A., . . . Fischer, M. (2007). *SIROCCO: Silent rotors by acoustic optimisation.* Paper presented at the Proceedings of the Second International Meeting on Wind Turbine Noise, September 20-21, Lyon, France.
Schust, M. (2004). Effects of low frequency noise up to 100 Hz. *Noise and Health, 6*(23), 73.
Serizel, R., Moonen, M., Wouters, J., & Jensen, S. H. (2012). A zone-of-quiet based approach to integrated active noise control and noise reduction for speech enhancement in hearing aids. *Audio, Speech, and Language Processing, IEEE Transactions on, 20*(6), 1685-1697.
Shepherd, D. G. (1990). Historical development of the windmill. *Cornell Univ. Final Report, 1*.
Son, E., Kim, H., Kim, H., Choi, W., & Lee, S. (2010). Integrated numerical method for the prediction of wind turbine noise and the long range propagation. *Current Applied Physics, 10*(2), S316-S319.
Sun, X., Kuo, S. M., & Meng, G. (2006). Adaptive algorithm for active control of impulsive noise. *Journal of Sound and Vibration, 291*(1), 516-522.
Swift-Hook, D. (1989). Wind energy and the environment. Peter Perengrinus Ltd, United Kingdom.
Tian, Y., Cotte, B., & Chaigne, A. (2013). *Wind Turbine Noise Modelling Based on Amiet's Theory.* Paper presented at the Proceedings of the 5th International Meeting on Wind Turbine Noise.

Tonin, R. (2012). Sources of wind turbine noise and sound propagation. *Acoustics Australia, 40*(1), 20-27.

Van den Berg, G. (2004). *Do wind turbines produce significant low frequency sound levels?*. Paper presented at the 11th International Meeting on Low Frequency Noise and Vibration and its Control Maastricht The Netherlands 30 August to 1 September 2004.

Wang, J., & Huang, L. (2006). Active control of drag noise from a small axial flow fan. *The Journal of the Acoustical Society of America, 120*(1), 192-203.

Wong, Y.-J., Paurobally, R., & Pan, J. (2003). Hybrid active and passive control of fan noise. *Applied Acoustics, 64*(9), 885-901.

Yang, I.-H., Jeong, J.-E., Jeong, U.-C., Kim, J.-S., & Oh, J.-E. (2014). Improvement of noise reduction performance for a high-speed elevator using modified active noise control. *Applied Acoustics, 79*, 58-68.

Zahedpour, S., Feizi, S., Amini, A., Ferdosizadeh, M., & Marvasti, F. (2009). Impulsive noise cancellation based on soft decision and recursion. *Instrumentation and Measurement, IEEE Transactions on, 58*(8), 2780-2790.

Zhu, R. (2009). *Active Control of Impulsive Noise.* Thesis for Masters degree, University of Minessota, Duluth .